Received: 4 June 2020 | Revised: 27 August 2020 | Accepted: 5 September 2020

DOI: 10.1002/er.6060

RESEARCH ARTICLE

INTERNATIONAL JOURNAL OF ENERGY RESEARCH WILEY

PEI modified natural sands of Florida as catalysts for hydrogen production from sodium borohydride dehydrogenation in methanol

Erk Inger[1] | Sahin Demirci[2] | Mehmet Can[2] | Aydin K. Sunol[3] | George Philippidis[4] | Nurettin Sahiner[2,3,5]

[1]Airframe and Powerplant Maintenance, Atilim University, Ankara, Turkey

[2]Department of Chemistry & Nanoscience and Technology Research and Application Center, Canakkale Onsekiz Mart University Terzioglu Campus, Canakkale, Turkey

[3]Department of Chemical and Biomolecular Engineering, University of South Florida, Tampa, Florida

[4]Patel College of Global Sustainability, University of South Florida, Tampa, Florida

[5]Department of Ophthalmology, Morsani College of Medicine, University of South Florida, Tampa, Florida

Correspondence
Nurettin Sahiner, Department of Chemistry & Nanoscience and Technology Research and Application Center, Canakkale Onsekiz Mart University Terzioglu Campus, Canakkale, Turkey.
Email: sahiner71@gmail.com; nsahiner@usf.edu

Summary

Sand samples from Tampa (T) and Panama (P) City beaches in Florida were used as catalysts for dehydrogenation of $NaBH_4$ in methanol. T and P sand samples were sieved to <250, 250 to 500, and >500 μm sizes, and the smallest fractions resulted in faster hydrogen generation rates (HGR), 565 ± 18 and 482 ± 24 mL H_2 (min.g of catalyst)$^{-1}$, respectively. After various base/acid treatments, HGR values of 705 ± 51 and 690 ± 47 mL H_2 (min g of catalyst)$^{-1}$ for HCl-treated T and P sand samples were attained, respectively. Next, T and P sand samples were modified with polyethyleneimine (PEI) that doubled the HGR values, 1344 ± 103, and 1190 ± 87 mL H_2 (min.g of catalyst)$^{-1}$ and increased ~8-fold, 4408 ± 187, and 3879 ± 169 mL H_2 (min g of catalyst)$^{-1}$, correspondingly after protonation (PEI^+). The Ea values of T and P sand samples were calculated as 24.6 and 25.9 kJ/mol, and increased to 36.1, and 36.6 kJ/mol for T-PEI^+ and P-PEI^+ samples, respectively.

KEYWORDS

H_2, $NaBH_4$ dehydrogenation, natural catalyst, renewable energy, sand catalyst

1 | INTRODUCTION

Greenhouse gas emissions from the use of fossil fuels continue unabated around the world raising concerns about climate change and the future of our planet. As a result, development of clean, renewable, and cost effective energy is being rigorously pursued around the world.[1] Although hydrogen (H_2) still faces challenges in terms of production and storage, it represents a promising clean form of energy, especially for transportation.[2-6] For H_2 storage, various materials such as sodium borohydride ($NaBH_4$),[7,8] magnesium borohydride ($Mg[BH_4]_2$),[9] lithium aluminum hydride ($LiAlH_4$),[10] ammonia borane (NH_3BH_3),[11,12] hydrazine (N_2H_4),[13,14] and hydrazine borane ($N_2H_4BH_3$)[15,16] have been proposed. Among them, $NaBH_4$ has received great interest due to its stability, H_2 density, easily controlled hydrogen generation rate (HGR), side product recyclability, and mild reaction conditions.[17-19] Solvents such as water, ethanol, methanol, and propylene glycol have been extensively investigated for the $NaBH_4$ dehydrogenation reaction.[20-23] Besides, diverse reaction pathways were utilized in H_2 generation including aluminum-water reaction in acidic and alkaline media,[24] photocatalytic hydrogen evolution,[25,26] and

bio-hydrogen production,[27] and so on. $NaBH_4$ dehydrogenation in methanol, as shown in Equation (1), offers several advantages in comparison to other solvents, such as high reaction rate at room temperature, H_2 production even in subzero temperatures thanks to the high freezing point of methanol, −97.6°C, and no requirement for a conventional metal-based catalyst.[28]

$$NaBH_4 + 4CH_3OH \rightarrow 4H_2 + NaB(OCH_3)_4 \quad (1)$$

The reaction requires the presence of a catalyst to achieve a high HGR for powering fuel cells. Several catalysts, such as metal nanoparticles[29-33] and polymeric ionic liquids[34-37] have been reported for $NaBH_4$ dehydrogenation in methanol. Along with performance, reusability, and regeneration ability, catalysts should also be sustainable and cost effective. As a result, there is interest in developing catalysts from natural resources, such as natural halloysite nanotubes (clay),[38,39] microgranular cellulose,[40] and carbon particle from lactose[41] and so on have been sought as benign catalyst to catalyze $NaBH_4$ dehydrogenation reaction in methanol.

In this study, we examined the use of inexpensive and renewable natural sand collected from the Tampa (T) and Panama City (P) beaches in Florida as catalysts for the $NaBH_4$ dehydrogenation reaction in methanol. Sands are inert materials and are mainly made up of SiO_2 in form of quartz. The "T" and "P" sand samples were tested in their natural form, as well as in processed form after washes with several acids, reaction with polyethyleneimine (PEI), and protonation. The effects of acid washing, amine modification, and protonation on HGR were measured and the reuse and regeneration of these sand catalysts for $NaBH_4$ dehydrogenation in methanol were investigated. The main motivation of this study is to demonstrate the usability of natural sands as cheap, abundant, easily accessible, and chemically modifiable alternative catalysts with laborless and repetitive utilization abilities for potential H_2 generation in wide range of industrial applications.

2 | EXPERIMENTAL METHODS

2.1 | Chemicals

Sand samples were obtained from Tampa (T) and Panama City (P) beaches in Florida (USA) about ∼20 m inland from the seawater. Sodium hydroxide (NaOH, 99.5%-100.5%, Sigma Aldrich), hydrochloric acid (HCl, 36.5%-38%, Sigma-Aldrich), nitric acid (HNO_3, ACS reagent 70% Sigma-Aldrich), sulfuric acid (H_2SO_4, ACS reagent 95%-97% Sigma-Aldrich), phosphoric acid (H_3PO_4, 85% Merck), acetic acid (CH_3COOH, 99.8%-100.5% Sigma-Aldrich), dimethylformamide (DMF, 99%, Merck), epichlorohydrin (EPC, 99%, Aldrich), PEI (50% in water Mn:1800, Sigma Aldrich), ethanol (99.8%, Sigma-Aldrich), and methanol (99.8%, Sigma-Aldrich) were used as received. Sodium borohydride ($NaBH_4$, 98%, Merck) was used as a H_2 source. Distilled water (DW, GFL 2108) was used throughout the experiments.

2.2 | Preparation of sand as catalyst

The preparation of T and P sand samples as catalysts was performed in accordance with the literature.[38] Briefly, the sand samples were sifted through sieves of 500 and 250 μm, and 15 g of each filtered T and P sand sample was washed in 500 mL of ethanol-water mixture (50:50 vol/vol) at 1500 rpm for 24 hours. Then, the washed T and P samples were washed with DW, ethanol, and acetone and dried in an oven at 50°C before serving as catalysts for $NaBH_4$ dehydrogenation in methanol.

Given that smaller catalyst size in general leads to better catalytic performance for a given material, the smallest size fractions of both T and P samples (particle size <250 μm) were treated with NaOH and various acids, namely HCl, HNO_3, H_2SO_4, H_3PO_4, and CH_3COOH, and then used as catalyst for $NaBH_4$ dehydrogenation to determine the effect of acid treatment on H_2 production. For this goal, 3.0 g of T and P samples were placed in 100 mL of 1M acid solution and stirred at 1400 rpm for 4 hours. Then, the sands were washed once with DW and acetone and dried in an oven at 50°C before testing them as catalysts.

Modifications of T and P sand samples were carried out by following the literature.[38] Briefly, 1.0 g of each sand sample was treated with 100 mL of 1M NaOH solution for 2 hours to activate their hydroxyl groups on the surface. Then, the treated T and P sand samples were washed two times with DW to eliminate excess NaOH. Subsequently, the samples were placed in 45 mL of 0.04M EPC solution in DMF at 90°C and stirred at 800 rpm for 1 hour. Finally, 3 mL of PEI solution in 5 mL DMF was added to the reaction medium and stirred at 90°C for 1 hour. Next, the PEI-modified sand samples T-PEI and P-PEI were washed once with DMF, DW, ethanol, and acetone. Finally, 1.0 g of the PEI-modified sand samples were treated with 100 mL of 1M HCl solution at room temperature for 2 hours to protonate their surface-attached amine groups. Finally, the obtained $T\text{-}PEI^+$ and $P\text{-}PEI^+$ sand samples were washed with DW and acetone, dried, and stored for subsequent use.

2.3 | Characterization

The FT-IR spectra of the T and P sand samples were recorded by using an FT-IR spectrometer (Thermo Nicolet iS10) equipped with attenuated total reflection (ATR) between 4000 and 650 cm^{-1}. Their thermal stabilities were compared via Thermo Gravimetric analysis (TG, SII TG/DTA 6300, EXSTAR) under a continuous nitrogen flow rate of 200 mL/min at a heating rate of 10°C/min from 75°C to 1000°C.

X-ray powder diffraction patterns of the T and P based sand samples were recorded by a PANalyticalX'Pert Pro MPD diffractometer equipped with CuKα radiation and the X'Celerator detector on diffracted beam. The XRD data were collected in a Bragg Brentano (θ/θ) vertical geometry operating in flat reflection mode between 3° and 70° (2θ) in steps of 0.02° 2θ with 1 second step-counting time. The X-ray tube operating at 45 kV and 40 mA was used and 1/2° divergence slit, a 0.04 rad soller slit and a 10 mm fixed mask was placed in the incident beam pathway. The High Score Plus (v.4.6.0) software was used for peak identification and automated search-match to analyze diffraction patterns. The quantitative analyses have been carried out by the combined Rietveld-Reference Intensity Ratio (R.I.R) method as explained by Young.[42]

The chemical compositions of the T and P sand samples were determined with an XRF spectrometer P analytical Axios Max. Samples were prepared as fused beads for XRF. Fused beads were prepared by mixing a finely powdered (<63 μm) sample and a flux (lithium tetraborate/metaborate mixture) with a ratio of 10:1 and then heated to 980°C ± 20°C in a platinum crucible. The powders were heated up to 1000°C for 1 hour to determine the loss of ignition as weight difference before and after heating.

2.4 | $NaBH_4$ dehydrogenation studies

The T and P sand samples and their PEI-modified and protonated forms were tested as catalysts for the $NaBH_4$ dehydrogenation reaction in methanol in a similar way as reported in the literature.[37,40] For the reactions, 50 mg of sand as catalyst and $NaBH_4$ (0.0965 g or 0.125 mM unless otherwise stated) were placed into a 50 mL flask that was attached to an inverted graded volumetric cylinder filled with water to quantify H_2 generation. After adding 20 mL of methanol to the reaction flask, the produced H_2 passed through a trap that contained concentrated H_2SO_4 to capture moisture and methanol and filled the volumetric cylinder for time progression measurements.

2.5 | Activation parameters

The activation energy E_a, enthalpy ΔH, and entropy ΔS values of the sand samples for the catalytic $NaBH_4$ dehydrogenation were calculated by running the reaction at the temperature range −20°C, −5°C, 10°C, 25°C, and 40°C using the well-established Arrhenius (2) and Eyring (3) equations:

$$\ln k = \ln k_0 - (E_a/\mathrm{RT}) \quad (2)$$

$$\ln(\mathrm{k/t}) = -(\Delta \mathrm{H/R})(1/\mathrm{T}) + \ln(\mathrm{kB/h}) + \Delta \mathrm{S/R} \quad (3)$$

where k_0 is the rate constant (mol/[min·g]), E_a is the activation energy (kJ/mol), R is the gas constant (8.314 kJ/[mol·K]), T is the reaction temperature (K), k_B is the Boltzmann constant (1.381×10^{-23} J K^{-1}), h is the Planck constant (6.626×10^{-34} J s), ΔH is the activation enthalpy (kJ/mol), and ΔS (J/mol K) is the activation entropy. The calculated E_a, ΔH, and ΔS values for T and P sand catalysts were compared to those reported in the literature.

2.6 | Reusability and regeneration studies

The reusability of T and P sand samples as catalysts for the $NaBH_4$ dehydrogenation reaction in methanol was studied by following the literature.[37,40] Accordingly, 50 mg of catalyst were placed in a 50 mL round bottom flask with 0.0965 g of $NaBH_4$. As soon as 20 mL of methanol were added into the reaction flask, H_2 production initiated. Upon termination of H_2 production, the same amount of $NaBH_4$, 0.0965 g, was added directly into the reaction media and the produced H_2 volume was recorded over time. Additional cycles of $NaBH_4$ dehydrogenation were repeated successively up to 10 times, and the HGRs were calculated to compare the activity and conversion of the reactions.

The regeneration performance of T and P sand samples was also studied by following the literature.[37,40] Specifically, after 50 mg of catalyst were employed in five consecutive reactions of $NaBH_4$ dehydrogenation in methanol, the flask contents were centrifuged and washed once with DW and then treated with 1M HCl for 2 hours to reprotonate the catalysts. Then, these HCl-treated catalysts were used in five sequential reactions of $NaBH_4$ dehydrogenation in methanol. This cycle was successively repeated five times and the activities of the catalysts were compared.

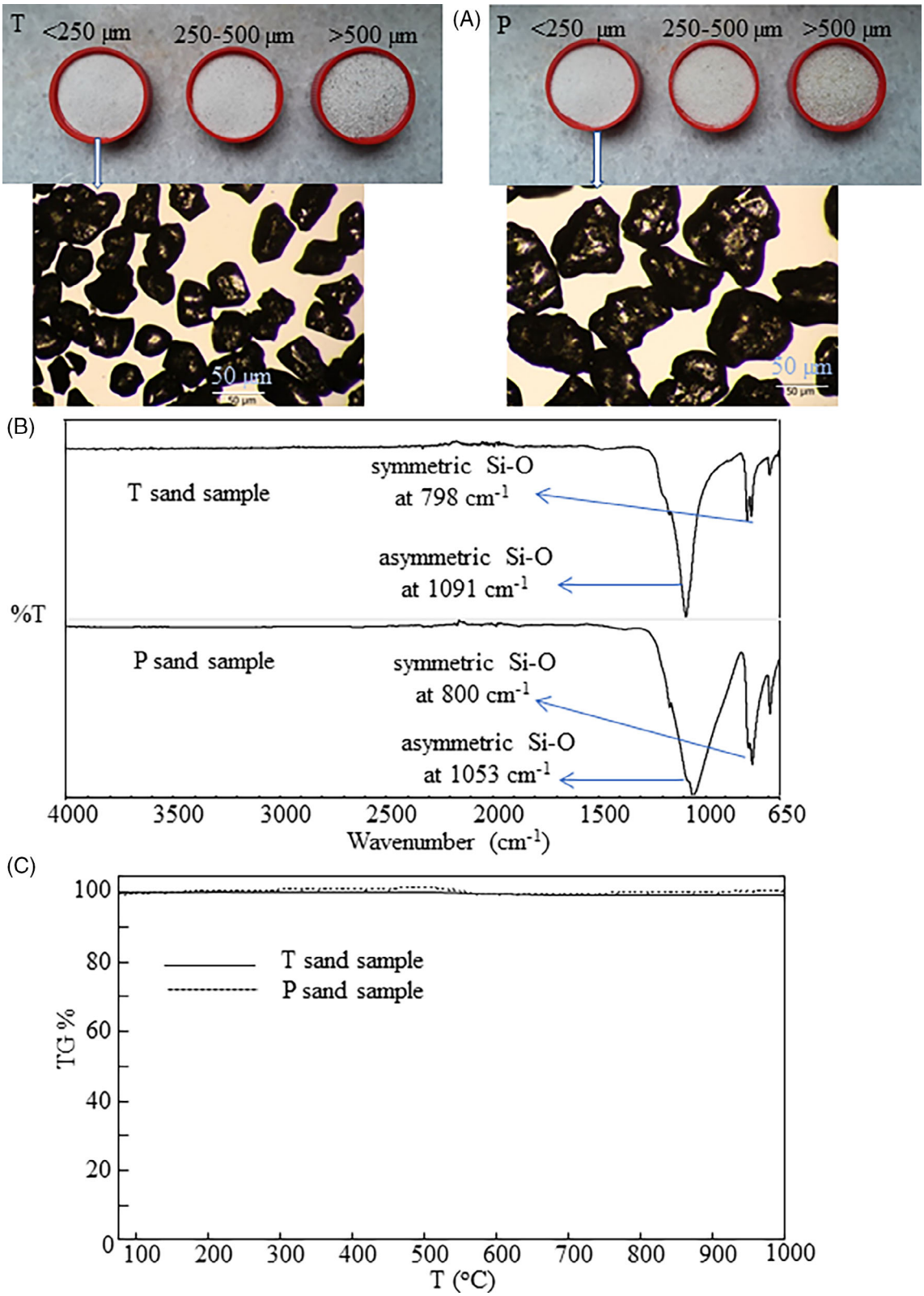

FIGURE 1 A, digital camera images; B, FT-IR spectra; and C, TGA thermograms of T and P sand samples [Colour figure can be viewed at wileyonlinelibrary.com]

3 | RESULTS AND DISCUSSION

3.1 | Characterization of sand samples

The functional group and thermal characterization of T and P sand samples were done by means of FT-IR and TG analysis. As illustrated in Figure 1A, the digital camera and optical microscopy images of T and P sand samples at different size ranges are white and as the size gets bigger, the color changes to yellowish. It is also apparent that the sand samples are irregularly shaped and coarse. The FT-IR spectra and thermograms are shown in Figure 1B,C, respectively. The characteristic absorption band at 1091 and 1053 cm^{-1} is due to asymmetric vibration of Si—O for the T and P sand samples, respectively. Similarly, the symmetric vibrations of Si—O at 798 and 800 cm^{-1} are in accordance with silica particle characteristic bands for T and P sand samples, respectively.[21]

The shifts in Si—O stretching frequencies for T and P samples can be attributed to their different locations that may have contributed different impurities to their structure. The thermograms are also presented in Figure 1C, where it is be clearly seen that there is no thermal degradation when heated up to 1000°C, implying absence of organic matter.

The surface area measurements for T and P based san samples were conducted by means of a flowing gas BET surface area analyzer (Micromeritics, TriStar II, Atlanta, GA), and the corresponding N_2 adsorption/desorption isotherms are provided in Figure S1A,B, respectively. According to the BET analyses, the T and P sand samples possess nonporous structures, or alternatively, the pore size of the sands might be in macroporous scales which is beyond the limits of multilayer gas adsorption analysis performed by BET method as it is used for microscale and mesoscale porosity measurements.

The XRD analysis revealed amorphous and quartz compositions of the T and P sand samples, and corresponding XRD patterns are given in Figure S2A,B, respectively. Accordingly, T samples were found to possess 1.3% amorphous and 98.7% quartz character whereas P sand samples are composed of 91.3% quartz and 8.7% amorphous phases. The peaks observed at 4.26, 3.34, 2.46, 2.24, and 2.13 °A confirm the quartz structure of T and P sand samples according to reference data fetched from Quartz COD database 9 010 144.

XRF analyses of the T and P sand catalysts were supportive of the obtained XRD data and are given in Table 1.

However, the presences of some residual minerals/impurities were also recorded. The T sands contained 95.5% SiO_2, 2.0% Al_2O_3, 0.8% TiO_2, 0.5% CaO, 0.2% Fe_2O_3, 0.1% P_2O_5, 0.09% K_2O, 0.04% MgO, and trace amount of Na_2O. The P sands on the other hand were found to be composed of 97.2% SiO_2, 2.4% Al_2O_3, 0.2% TiO_2, 0.08% Fe_2O_3, 0.08% P_2O_5, 0.04% K_2O, 0.03% MgO, and trace amount of CaO and Na_2O minerals.

TABLE 1 XRF analysis result for T and P sand samples

	Material (Sand sample)	
Content (%)	**T**	**P**
SiO_2	95.47	97.22
Al_2O_3	1.97	2.40
TiO_2	0.78	0.18
Fe_2O_3	0.16	0.08
CaO	0.52	Trace
MgO	0.04	0.03
Na_2O	Trace	Trace
K_2O	0.09	0.04
ZrO_2	0.21	-
P_2O_5	0.14	-

3.2 | Catalytic studies

The catalytic performance of the T and P sand samples were tested during $NaBH_4$ dehydrogenation reactions taking place in methanol to produce H_2. The T and P sand samples in the size ranges <250, 250 to 500, and >500 μm were used as catalysts and their H_2 production performance was compared. As smaller particles generally generate faster reaction kinetics, T and P sand samples with <250 μm size used as catalyst were compared to self-methanolysis of $NaBH_4$ as illustrated in Figure 2A. The $NaBH_4$ self-dehydrogenation in methanol without catalyst came to conclusion in 35 minutes with 250 ± 2 mL of H_2 produced, which represents a 100% conversion according to Equation (1). The use of T and P sand samples at <250 μm size as catalysts for $NaBH_4$ dehydrogenation reduced to 20 and 24 minutes, respectively, the time needed to reach full conversion. Differences in the composition of T and P sand samples may be the main reason for slight differences in their catalytic activities against H_2 production from $NaBH_4$ in methanol.

To determine the effect of sand particle size on the HGR, expressed in mL H_2(min g of catalyst)$^{-1}$, the HGR values of the T and P sand fractions of <250, 250 to 500, and >500 μm were compared, as illustrated in Figure 2B. The HGR values are calculated based on the time required to produce 125 mL of H_2. Overall, T sand samples exhibited higher HGR values than P samples of the same size range. As expected, the smallest size

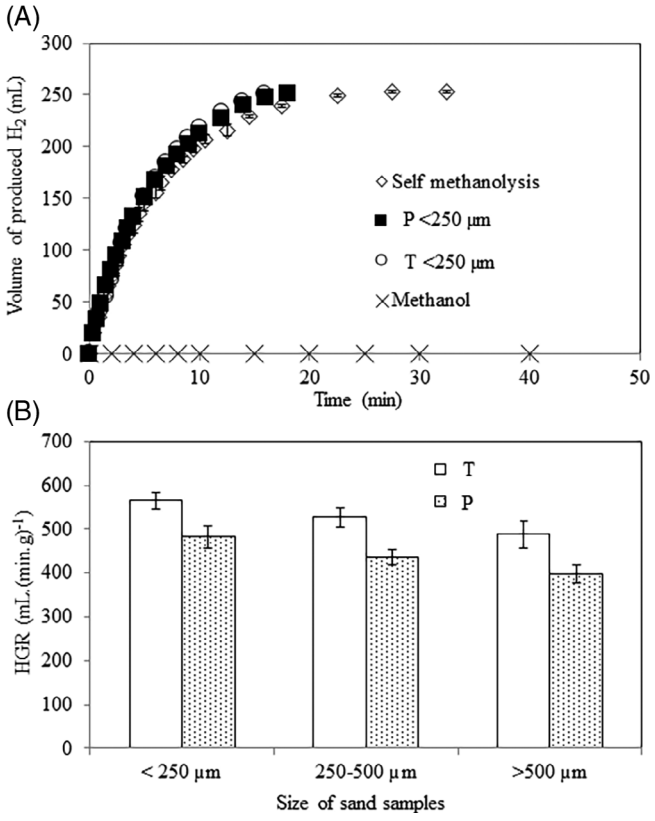

FIGURE 2 A, The comparison of the catalytic performance of T and P sand samples and with <250 µm with self-methanolysis of NaBH4 dehydrogenation; and B, the effect of NaOH and different acid treatments on Hydrogen generation rate values of T and P sand samples as catalyst for NaBH4 dehydrogenation in methanol [Reaction conditions: 50 mg of catalyst, 125 mM NaBH4 in 20 mL of methanol, 25°C, 1000 rpm]

fractions of T and P sand samples (<250 µm) showed the highest HGR values of 565 ± 18 and 482 ± 24 mL H_2(min g of cat)$^{-1}$). The HGR values of the 250 to 500 µm and > 500 µm fractions of T sand samples were calculated to be 527 ± 22, and 489 ± 31 mL H_2(min.g of catalyst)$^{-1}$), whereas those for the corresponding fractions of the P sand samples were 436 ± 17 and 397 ± 21 mL H_2(min g of catalyst)$^{-1}$. Therefore, the smallest size of T and P sand samples, <250 µm, was chosen for further studies via treatment with NaOH and the acids HCl, HNO_3, H_2SO_4, H_3PO_4, and CH_3COOH in an effort to increase the HGR values of these natural catalysts.

The effect of NaOH and various acid treatments on the catalytic performances of T and P sand samples was studied and the findings are shown in Figure 3A. The HGR values for NaOH-, HCl-, HNO_3-, H_2SO_4-, H_3PO_4-, and CH_3COOH-treated T sand samples catalyzing the $NaBH_4$ dehydrogenation reaction were calculated to be 542 ± 13, 705 ± 51, 628 ± 29, 621 ± 33, 624 ± 28, and 626 ± 32 mL H_2(min g of catalyst)$^{-1}$), respectively. The HGR values for NaOH, and acid treated P sand samples were found as 550 ± 11, 690 ± 47, 600 ± 21, 599 ± 19, 601 ± 24, and 587 ± 17 mL H_2(min g of cat)$^{-1}$ in the same respective order. As both of the HCl-treated T and P sand samples showed higher HGR values among the treated samples, their time progression of H_2 production was compared to those of the bare sand samples, as seen in Figure 3B,C, respectively.

The $NaBH_4$ dehydrogenation reaction using HCl-treated T and P sand samples were completed in 16 and 18 minutes, respectively, which were 20% faster than the bare T and P sand catalysts for the same reaction. These results are in agreement with the literature as many other types of acid-treated catalysts have been reported to have higher catalytic activities for $NaBH_4$ dehydrogenation reaction in methanol.[21,30,43,44] The mechanism of $NaBH_4$ dehydrogenation reaction in water with hydroxyl groups-containing catalysts has been elucidated by many researchers.[45,46] The proposed reaction mechanism for hydroxyl groups containing catalysts (Silica particles etc) catalyzed $NaBH_4$ dehydrogenation reaction in methanol is depicted in Figure S3. It is known that the protic hydroxyl groups on the surface of catalysts interact with $[BH_4]^-$ generating —O—BH_3 linkage and releasing H_2. Then, the remaining three hydrogen of BH_3 are expected to undergo dehydrogenation by interaction with methanol molecules in solution, thus releasing H_2 via the Michaelis-Menten mechanism, as reported in literature.[45-47] Specifically, the generated —O—BH_3 on the catalyst surface would be turned to —O—B-$(OCH_3)_3$ in methanol and finally the interaction of —O—B-$(OCH_3)_3$ with one free methanol molecule in solution would lead to generation of the $[B(OCH_3)_4]^-$ as by-product, freeing the catalytic domain of the catalyst and re-establishing the original form of catalyst with functional —OH groups on the surface. As the reaction progresses, increasing amounts of $[B(OCH_3)_4]^-$ may accumulate on the surface of catalyst causing a reduction in the catalytic performance. On the other hand, the FTIR spectra of the sands revealed that both of the sand samples were devoid of hydroxyl groups. Since the hydroxyl groups play a key role in initiation of $NaBH_4$ dehydrogenation reaction in methanol, the observed very low catalytic activity of the sands were attributable to the lack of hydroxyl groups in the structure. Given that the HCl treatment of the T and P sand samples resulted in a rather negligible increase in HGR compared to bare sands, and self-methanolysis of $NaBH_4$, T and P sand samples were modified through reaction with PEI, a well-known amine source, as an alternative to acid treatment. The schematic depiction of PEI modification of sand particles is illustrated in Figure 4.

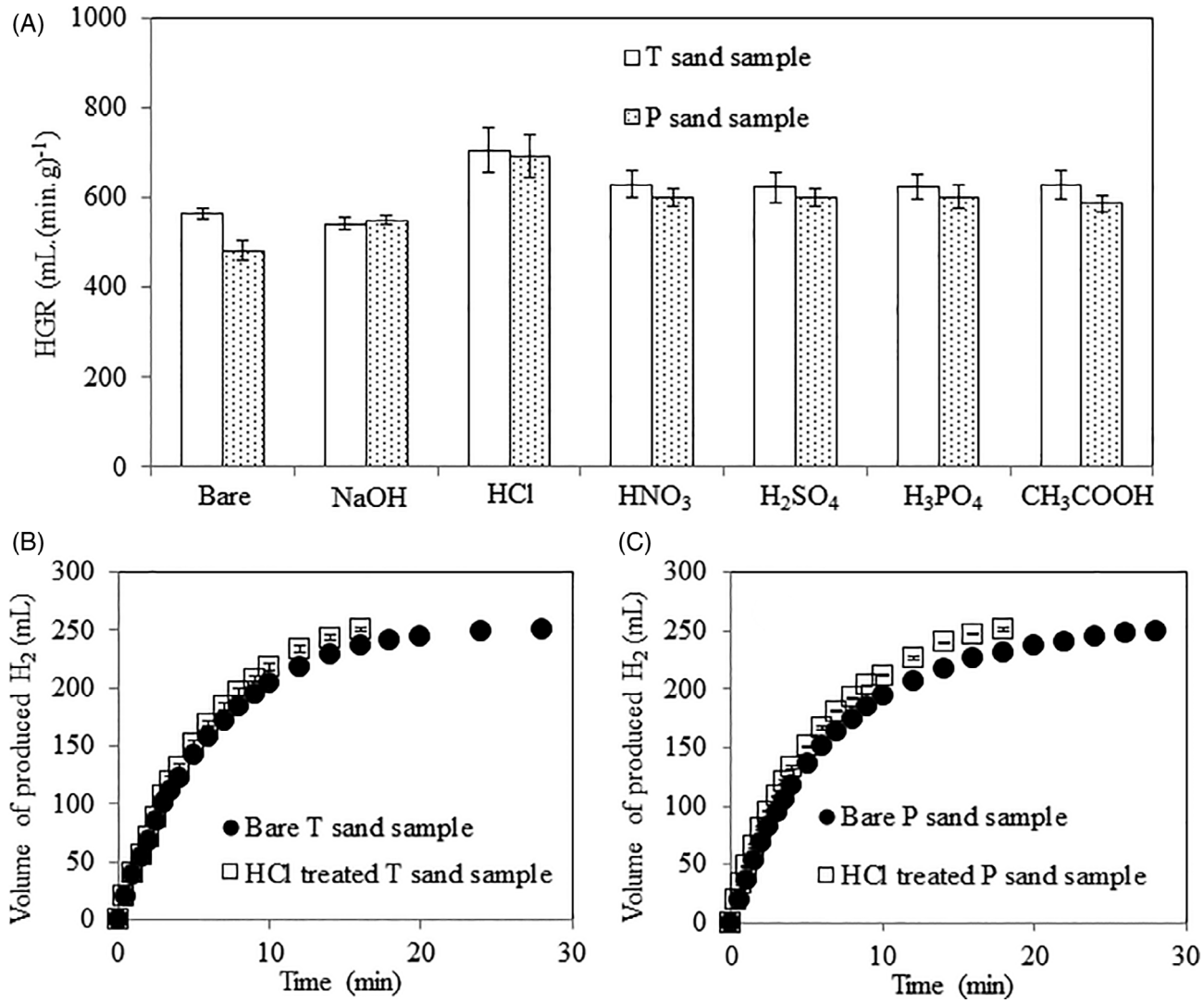

FIGURE 3 A, Hydrogen generation rate (HGR) values of T and P sand samples with different sizes; B, T; and C, P sand samples as catalyst for H2 production from NaBH4 dehydrogenation (reaction conditions: 50 mg of catalyst, 125 mM NaBH4 in 20 mL of methanol, 25°C, 1000 rpm)

The PEI modification of T and P sand samples was carried out in two steps by following the literature.[38] In the first step, NaOH treated T and P sand samples were reacted with EPC in DMF solution resulting in EPC getting covalently bonded to activated oxygen moieties on the surface of sand particles by ring opening of the epoxy groups. Afterward, when PEI was added, its amine groups bonded to EPC by displacing the Cl atoms. Finally, the prepared T-PEI and P-PEI sand samples were treated with 100 mL of 1M HCl solution to protonate the amine groups in an effort to further increase the positive charge of the catalysts.

The FT-IR spectra and TGA thermograms of PEI modified T and P sand samples are shown in Figure 5. The FT-IR spectra of bare T and T-PEI sand samples are compared in Figure 6A. The distinct peaks at 2986 and 2853 cm^{-1} are attributed to the aliphatic —CH_2 groups of the PEI, whereas the peaks at 1612 and 1489 cm^{-1} are attributed to N—H bending frequencies of the PEI molecules, thus confirming the modification of T sand samples. Similar peaks at 2974 and 2868 cm^{-1} for aliphatic —CH_2 groups and 1603, and 1472 cm^{-1} for N—H bending vibrations were also observed for PEI-modified P sand samples and the corresponding FTIR spectrum is shown in Figure 5B.

Moreover, the TGA thermograms shown in Figure 5C,D also confirm the PEI modification of the T and P sand samples with 25% and 27% weight loss at 1000°C, respectively, whereas there were no weight loss observed for bare T and P sand samples at the same temperature. Digital camera images of T and P sand samples, bare and after PEI modification and protonation, are

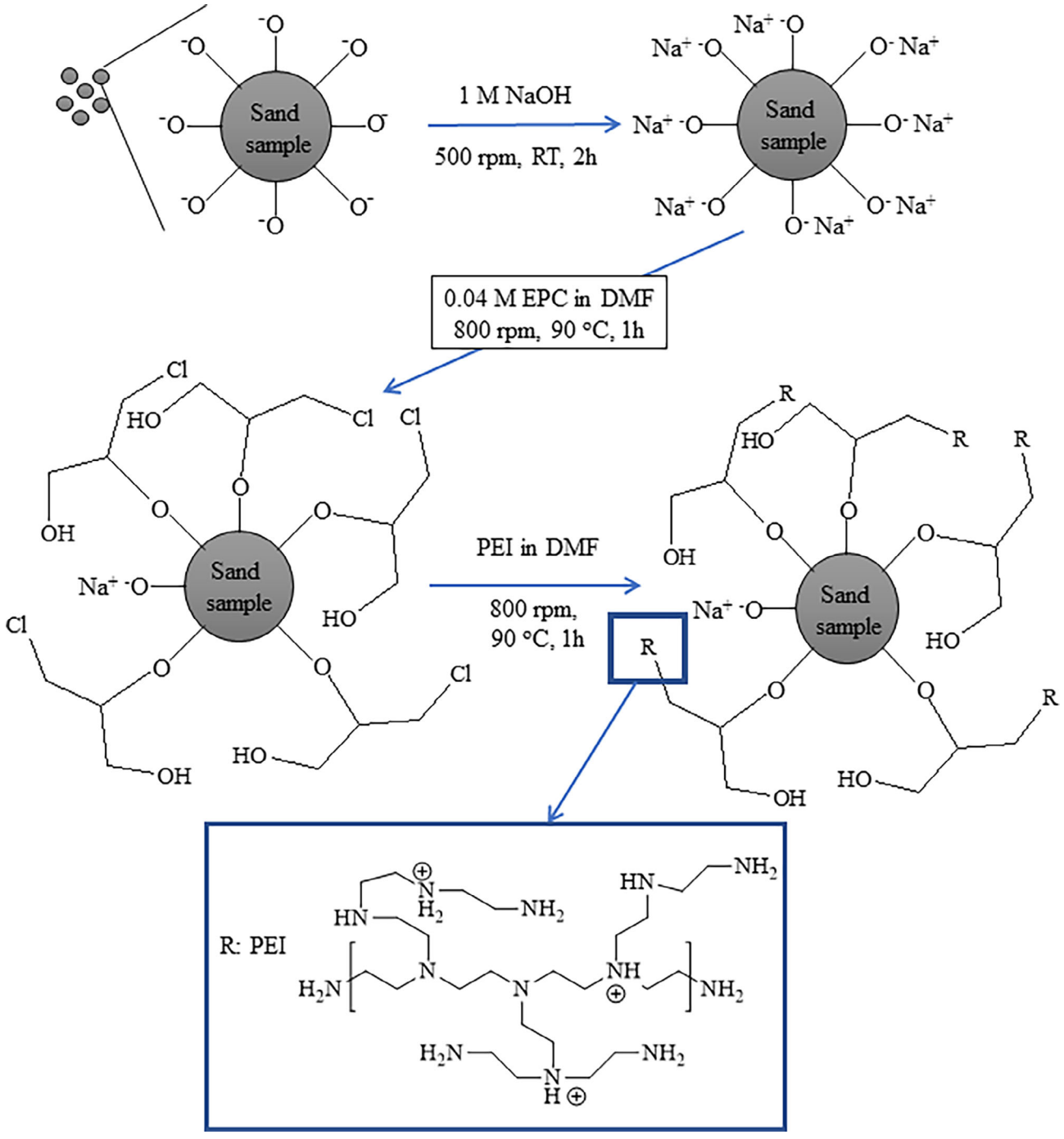

FIGURE 4 Schematic depiction of polyethyleneimine modification of T and P sand [Colour figure can be viewed at wileyonlinelibrary.com]

provided in Figure 5E. The white color of the bare T and P sand samples turned to yellowish and brownish after the PEI modification and protonation, respectively.

The XRD patterns of T-PEI$^+$, and P-PEI$^+$ sand samples were given in Figure S4A,B. The quartz structure of T and P sand samples were observed to decrease up to 50.4, and 83.4% from 98.7% and 91.3%, respectively after PEI modification. Subsequently, after the protonation process of T-PEI$^+$ and P-PEI$^+$ sand samples, 49.6, and 16.3% amorphous structures were noted from their XRD patterns. The amorphous structure of sand catalysts was expected to be imparted by PEI modification. Additionally, based on their percentile amorphous contents, one can obviously notice that, the efficiency of PEI modification for T sands was more than that of the T catalysts.

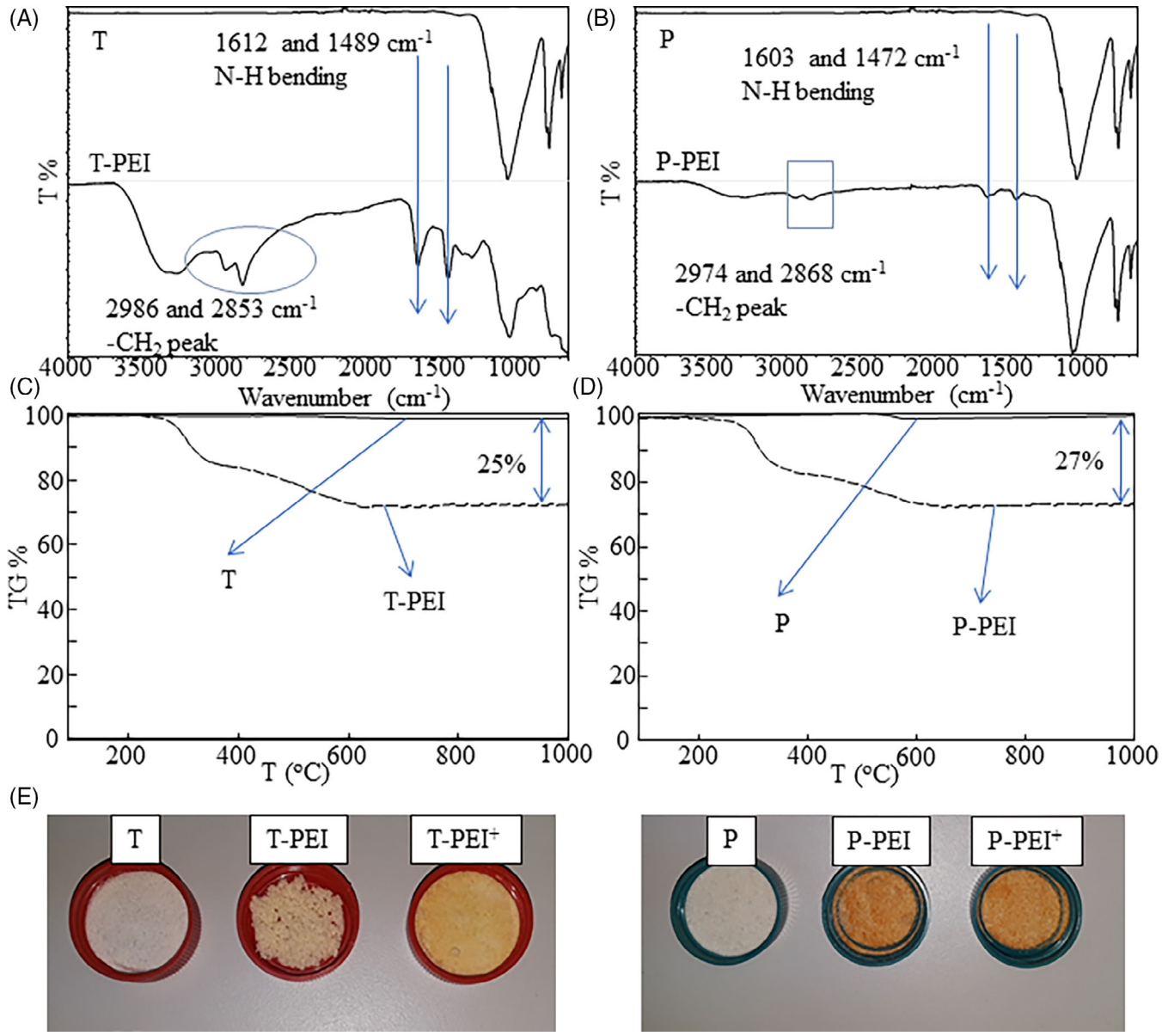

FIGURE 5 The FT-IR spectra of (A) T-PEI, (B) P-PEI sand samples, TGA thermograms of (C) T-PEI, (D) PPEI, and (E) digital camera images of bare and PEI modified T and P sand samples [Colour figure can be viewed at wileyonlinelibrary.com]

The catalytic effect of the PEI-modified and protonated forms of T and P sand samples on $NaBH_4$ dehydrogenation reactions in methanol were investigated, as shown in Figure 6. The timely progression of H_2 production by the T (bare), T-PEI, and T-PEI$^+$ sand samples can be seen in Figure 6A. Clearly, the rate of the reaction increased significantly upon PEI modification and protonation of the T sand samples. The dehydrogenation of $NaBH_4$ was completed in 16 minutes during T sand catalysis, whereas in the presence of T-PEI and T-PEI$^+$ the reaction was completed in 8 and 2.3 minutes, respectively. Similar results were observed with P, P-PEI, and P-PEI$^+$ catalyzed dehydrogenation of $NaBH_4$ in methanol, as shown in Figure 6B, with the reaction being completed in 18, 9, and 2.8 minutes in the presence of P, P-PEI, and P-PEI$^+$ sand samples, respectively. PEI molecules and their protonated forms (PEI$^+$) were also tested for their catalytic activity on $NaBH_4$ dehydrogenation reaction in methanol and obtained data was added to H_2 generation graphs in Figure S5. $NaBH_4$ dehydrogenation reaction in methanol catalyzed by PEI and PEI$^+$ molecules were respectively terminated at 52 and 3 minutes with approximately 245 mL of H_2 production. As can be extrapolated from these findings, H_2 production rates of PEI and PEI$^+$ molecules alone were drastically lower than PEI modified and protonated sand catalysts. Incorporation of PEI molecules to T and P sands presumably created more stable active sites on T and P sand samples

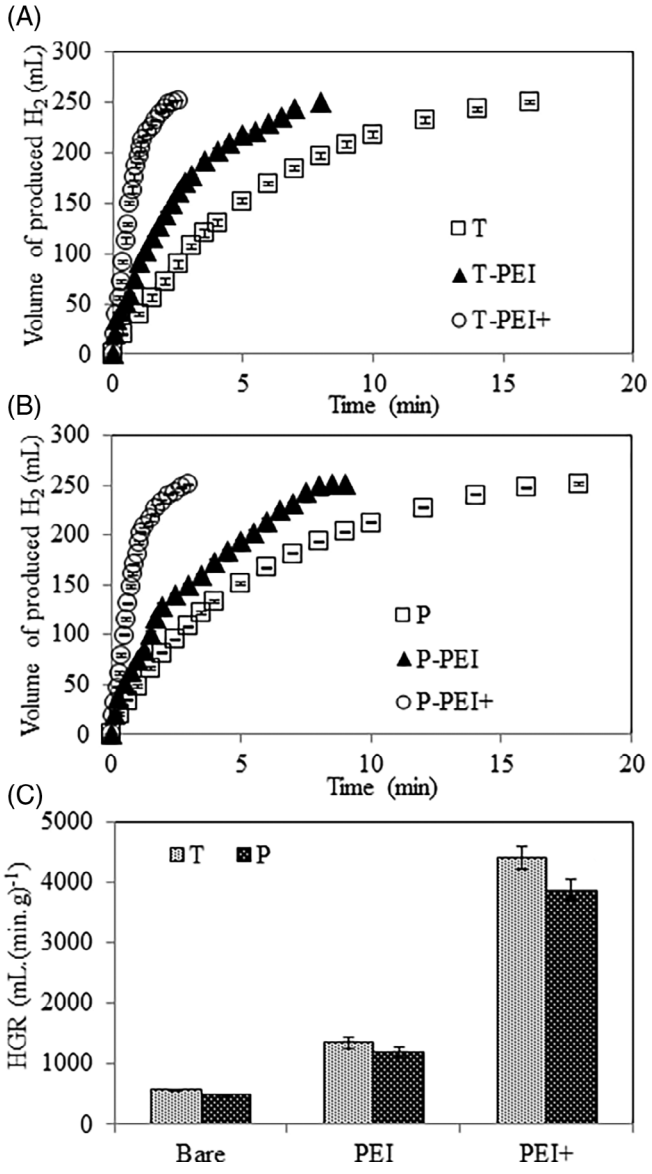

FIGURE 6 Comparison of the catalytic performance during NaBH4 dehydrogenation in methanol of A, T, TPEI, and T-PEI+ sand samples; B, P, P-PEI, and P-PEI+ sand samples; and C, hydrogen generation rate (HGR) values for T and P sand samples and their PEI-modified-protonated forms (Reaction conditions: 50 mg of catalyst, 125 mM NaBH4 in 20 mL of methanol, 25°C, 1000 rpm)

promoting higher catalytic activities than their constituents alone.

The HGR values calculated based on 50% reaction completion (125 mL of H_2 produced) are shown in Figure 6C. The HGR values for T sand samples were 565 ± 18, 1344 ± 103, and 4408 ± 187 mL H_2(min g of catalyst)$^{-1}$ for T, T-PEI, and T-PEI$^+$, respectively. Likewise, the HGR values for P, P-PEI, and P-PEI$^+$were 482 ± 241 190 ± 87, and 3879 ± 169 mL H_2(min g of catalyst)$^{-1}$, respectively. It should be noted that there was an almost eightfold increase in HGR of both T and P sand catalysts upon PEI modification and protonation. The increase in HGRs of PEI modified T and P sand catalysts can be attributed to protonation of amine groups by HCl formed in the course of PEI modification. Specifically, bonding of amine groups of PEI molecules to EPC-modified sand catalysts by displacing the Cl atom of EPC results in formation of HCl which in turn protonates some of the amine groups in the PEI chains and give rise to better catalytic activity in comparison to HCl treated, and untreated bare sand catalysts. Moreover, upon HCl treatment of PEI modified catalysts; fully protonated amine groups of PEI molecules give rise to faster H_2 generation, hence higher HGR values.

The proposed mechanism of PEI modified catalysts during dehydrogenation of $NaBH_4$ is illustrated in Figure S6. According to it, the protonated amine groups on the catalyst surface interact with borohydride anions (BH_4^-) and H_2 is released. Then, hydrogen atoms of the produced borane molecules (BH_3) react with methanol and H_2 gas is released. The reaction proceeds until all hydrogens from the borane molecule are removed. In the final step, the last product, trimethoxy borate $B(OCH_3)_3$ reacts with a methanol molecule to create $^-B(OCH_3)_4$,- while the catalyst returns to its original form to react with more $NaBH_4$ molecules.[48]

3.3 | Effect of temperature on $NaBH_4$ dehydrogenation

As catalytic performance in general depends on the reaction temperature, the catalytic activities of HCl-treated and PEI-modified-protonated T and P sand samples were tested at range of reaction temperatures −20°C, −5°C, 10°C, 25°C, and 40°C. The HGR values of HCl-treated sand samples at each reaction temperature are shown in Figure 7.

As expected, the HGR values increased significantly as the reaction temperature was raised. For HCl-treated T sand samples in Figure 7A, HGR increased from 93 ± 7 to 1065 ± 86 mL H_2 (min.g of catalyst)$^{-1}$, when the reaction temperature was raised from −20°C to 40°C, respectively. For the same temperature range, HCl-treated P sand samples showed an HGR increase from 75 ± 9 to 1111 ± 99 mL H_2 (min.g of catalyst)$^{-1}$. The calculated HGR values of the T-PEI$^+$, and P-PEI$^+$catalysts are compared in Figure 7B. The HGR values of T-PEI$^+$ were in general higher than those of P-PEI$^+$at all tested temperatures. Moreover, the HGR values of T-PEI$^+$ and P-PEI$^+$ catalyzed reactions were at least threefold higher than the HGR values of HCl-treated T and P sand samples at each tested temperature. Hence, PEI modification and

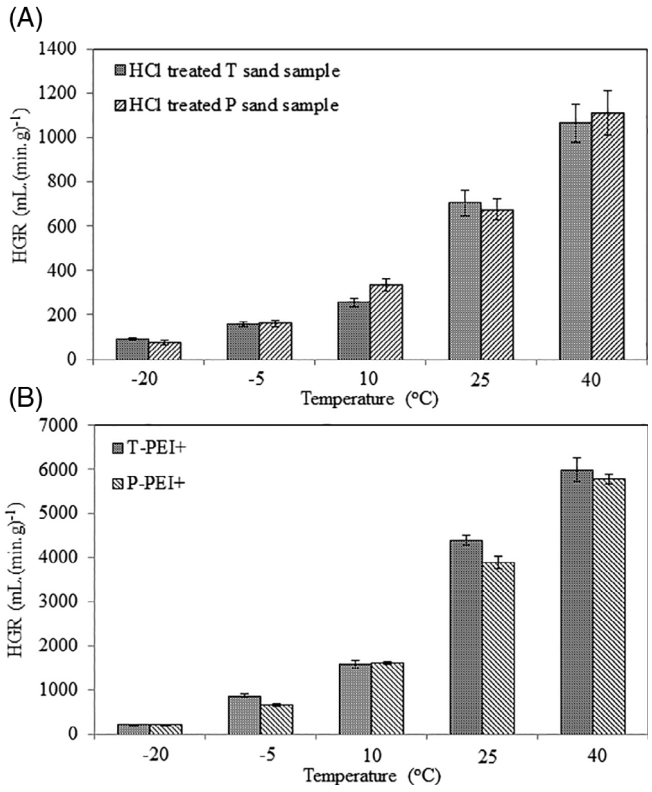

FIGURE 7 Comparison of hydrogen generation rate (HGR) values for A, HCl-treated T and P sand samples; and B, T-PEI+ and P-PEI+ during NaBH4 dehydrogenation in methanol at various temperatures (Catalyst: 50 mg, 20 mL 125 mM NaBH4, 1000 rpm mixing rate)

protonation of T and P sand samples leads to a significantly higher catalytic activity for H_2 production from dehydrogenation of $NaBH_4$ in methanol.

3.4 | Activation parameters

The E_a, ΔH, and ΔS values of HCl-treated and PEI-modified-protonated T and P sand samples were calculated from the ln(k) vs 1/T plots (Arrhenius eq.) and ln(k/T) vs 1/T plots (Eyring eq.), and the respective graphs are presented in Figure 8. The Arrhenius plots for HCl-treated T and T-PEI$^+$ sand catalyzed dehydrogenation reactions are presented in Figure 8A, whereas those for HCl-treated P and P-PEI$^+$ sands are shown in Figure 8B.

The Eyring plots for HCl-treated T and T-PEI$^+$ catalysts are shown in Figure. 8C, whereas those for HCl-treated P and P-PEI$^+$ sand samples are shown in Figure 8D. Strong R^2 values in excess of .97 were obtained in all those graphs. The activation parameters for both T and P catalysts were readily calculated from the Arrhenius and Eyring plots and were listed in Table 2. The E_a value for dehydrogenation of $NaBH_4$ in methanol without a catalyst was calculated as 62.9 kJ/mol.[49] The E_a, ΔH, and ΔS values for HCl-treated T sand catalyzed reaction was 24.6 kJ/mol, 21.8 kJ/mol, and −185 J/mol K, respectively, whereas for HCl-treated P sand the corresponding figures were 25.9 kJ/mol, 23.1 kJ/mol, and −180 J/mol K. Moreover, the E_a, ΔH, and ΔS values for T-PEI$^+$ and P-PEI$^+$ sands catalyzed dehydrogenation reactions were 36.1 kJ/mol, 32.9 kJ/mol, and −159 J/mol K, and 36.6 kJ/mol, 33.4 kJ/mol, and −158 J/mol K, respectively. These findings clearly indicate that the E_a values of HCl-treated T and P sand samples are similar to each other and lower than the E_a values of T-PEI$^+$, and P-PEI$^+$ catalysts. The activation parameters for HCl-treated and PEI-modified-protonated sand catalysts were compared to values for other catalysts from the literature as summarized in Table 2.

The E_a values of HCl-treated and PEI-modified-protonated T and P sand are lower than those reported for several metal catalysts, such as Ru/Al_2O_3 nanoparticles,[50] Ru_5Co/C,[31] Co-P/CNTs-Ni foam,[32] L-Proline-functionalized Rh nanoparticles,[51] and Ru-Ni/Ni foam.[36] Furthermore, metal-free catalysts, such as and HCl-SiO_2 also have a higher Ea value than the HCl-treated T and P sand samples.[21] On the other hand, there are several metal catalysts with lower E_a values, such as SO_4^{2-}/CuO,[52] Fe-B,[29] Co-TiO_2 nanoparticles,[30] and Ag@CFC particles.[53] Considering the industry's interest in low activation energy catalysts that are naturally abundant and environmentally friendly, the T and P sands merely treated with HCl seem to have strong potential for use in methanolysis of $NaBH_4$in future fuel applications.

3.5 | Reusability and regeneration capability of sands as catalyst

The reuse, regeneration, and chemical stability of catalysts are significant parameters for commercial consideration in terms of cost effectiveness. Reusability studies were conducted by using 50 mg of HCl-treated T and P sand catalysts 10 times consecutively for $NaBH_4$ dehydrogenation in methanol by adding 0.0965 g of $NaBH_4$ after cessation of each reaction. The reusability results of HCl-treated T and P sand samples are demonstrated in Figure 9A,B, respectively. Conversion was calculated based on the stoichiometry of Equation (1) and activity was calculated from the reaction rates calculated from H_2 production graphs.

Full conversion was achieved for both HCl-treated T and P sand samples in each of the 10 reuse cycles. Additionally, the activity of HCl-treated T sand samples was 100% in the first three uses (cycles), 99.8 ± 0.1% in the

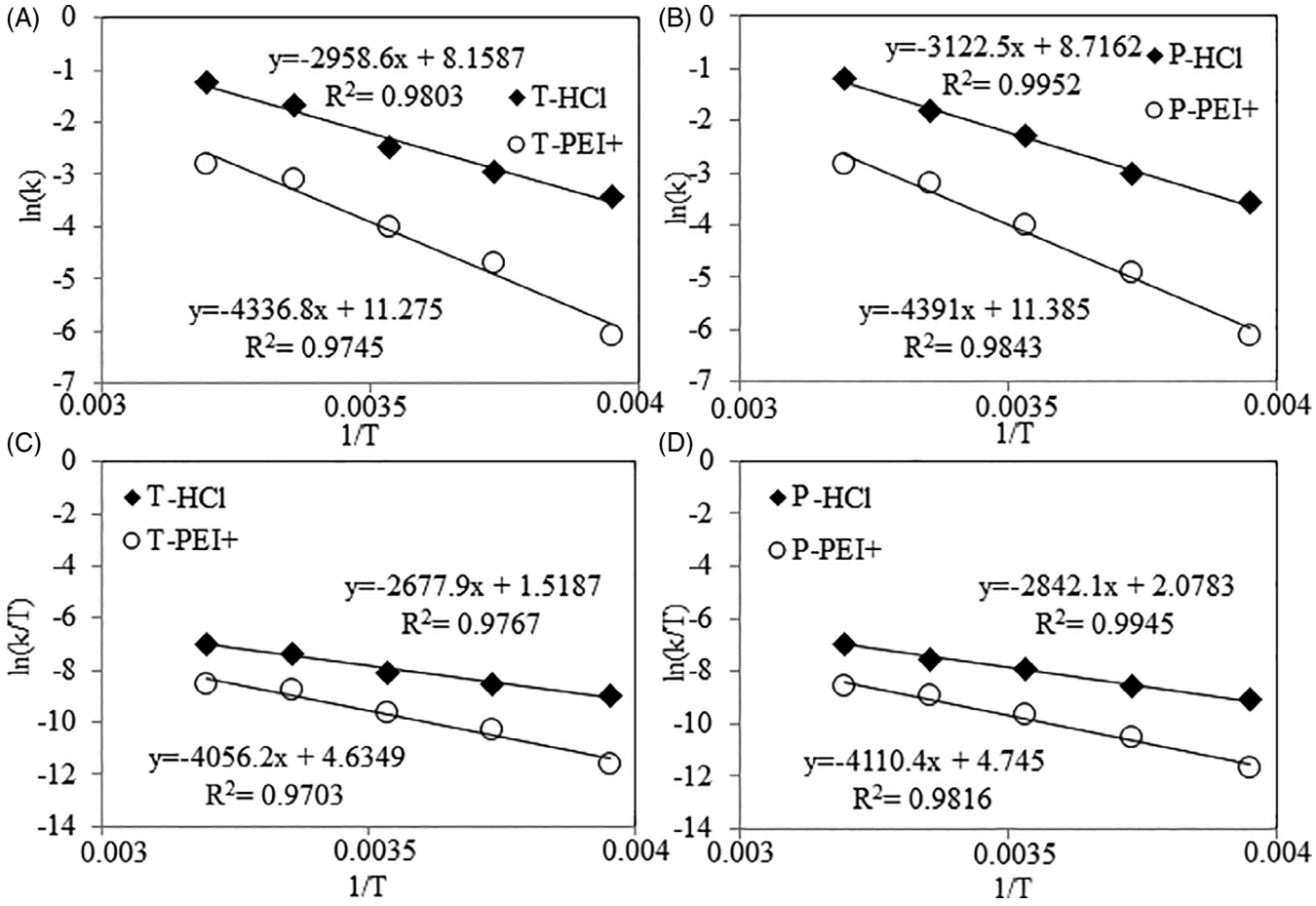

FIGURE 8 The ln k vs $1/T$ (Arrhenius eq.) plots of (A) T based, and (B) P based sand samples, and ln (k/T) vs $1/T$ (Eyring Eq.) plots of (C) T based, and (D) P based sand samples (50 mg catalyst, 20 mL 125 mM NaBH4 at 1000 rpm mixing rate)

fourth use, 99.2 ± 0.6% in the fifth use, and then decreased to 91.2 ± 3.9%, 79.5 ± 5.4%, 70.9 ± 7.2%, 68.3 ± 3.2%, and 67.4 ± 5.9% in the sixth through 10th use, respectively. Similarly, the activity of HCl-treated P sand samples was 100% in the first three usages, 98.2 ± 1.1% in the fourth use, and then decreased to 90.4% ± 3.2%, 82.9% ± 3.9%, 73.2% ± 5.4%, 70.3% ± 7.2%, 68.8% ± 3.2%, and 64.6% ± 5.9% in the fifth through 10th use, respectively, respectively. As both catalysts successfully achieved 100% conversion for every use in 10 consecutive runs with just about 30% reduction in activity, the practicality of these sand catalysts appears to be promising. The decrease in activity after 10 consecutive uses can be explained by the formation of sodium tetramethoxyborate ($NaB(OCH_3)_4$) as a by-product on the catalyst's surface, causing an inhibitory effect on H_2 production that is in accordance with the suggested reaction mechanism in Figure S3.

Similar reusability studies were conducted with T-PEI$^+$, and P-PEI$^+$ sand samples by using 50 mg of catalyst in five sequential reactions of the $NaBH_4$ dehydrogenation in methanol at the conditions mentioned above. The findings are shown in Figure 9C,D. The reusability of T-PEI$^+$, and P-PEI$^+$ catalysts was not as good as that of HCl-treated T and P sand samples. Nevertheless, 100% conversion was preserved for both T-PEI$^+$ and P-PEI$^+$ catalyzed dehydrogenation reactions for each of the five reuse cycles. The activity of the T-PEI$^+$ catalyst was 100% for first usage and then decreased to 97.4% ± 2.1%, 67.2% ± 4.1%, 66.6% ± 3.4%, and 56.9% ± 2.9% after the second through fifth use, respectively, as shown in Figure 9C.

The activity of the P-PEI$^+$ catalyst, as shown in Figure 9D, was 100% in the first cycle and decreased to 98.9% ± 2.1%, 95.4% ± 3.4%, 86.9% ± 2.1%, and 70.6% ± 5.3% in the second through fifth cycle, respectively. This decrease in catalytic activity can be explained as stated earlier. Moreover, activity of the catalysts can be retrieved upon treatment with HCl, and regenerated catalysts can be used in subsequent H_2 production reactions.

The regeneration capability of HCl-treated T and P sand samples is shown in Figure 10A,B, respectively. After 10 successive uses, each sand catalyst was treated with 1M HCl and was then used again in another

TABLE 2 Calculated activation parameters, HGR, and FOM values of the T and P sand samples and values reported in the literature for various other catalysts pertaining to $NaBH_4$ dehydrogenation reaction in methanol

Materials	Activation parameters			HGR (min^{-1})	Substrate/solvent ratio wt%	FOM[a] (1/(min. [$NaBH_4$].g_{cat}))	References
	E_a (kJ/mol)	ΔH (kJ/mol)	ΔS (J/mol.K)				
$NaBH_4$ dehydrogenation without catalyst	62.9	-	-	5	-	49	
HCl treated T sand sample	24.6	21.9	-185	705	0.5	10.0	This study
HCl treated P sand sample	25.9	23.1	-180	690	0.5	8.9	This study
T-PEI^+	36.1	32.9	-159	4408	0.5	69.6	This study
P-PEI^+	36.6	33.4	-158	3879	0.5	57.1	This study
HCl-SiO_2	29.9			34000	0.5	11.4	21
Ru/Al_2O_3	51.0	-	-	204	1	-	50
Ru_5Co/C	36.8	-	2250	10	0.6	31	
Co-P/CNTs-Ni	49.9	-	-	2430	10	-	32
SO_4^{2-}/CuO	13.1	-	-	965	2	22.7	52
Fe-B	7.02	-	-	198	10	-	29
Co-TiO_2	20.4	-	-	144000	3.4	-	30
P/boehmite	21.6	-	-	-	5	-	34
p(2-VP)$^{++}C_6$	20.8	-	-	1664	0.5	16.0	35
Ru-Ni/Ni	39.9	-	-	360	15	-	36
Ni_2P-TOP	19.4	-	-	8110	1	43.8	37
Cell-EPC-DETA-HCl	23.7	-	-	3215	0.5	53.3	38
L-Proline-functionalized Rh	38.2	-	-	-	0.5	-	51
CF-A-CH	14.4	-	-	1179	2.5	10.2	47
Ag@CFC	20.1	-	-	2049	0.15	8.3	53

[a]FOM values were calculated from reported informations from according papers.
Abbreviations: HGR, hydrogen generation rate; LOM, figure of merit.

10 consecutive dehydrogenation reactions, so this reuse-regeneration cycle was repeated a total of four times. The HCl-treated T and P sand activity values for the 1st and 10th use of each cycle is shown in Figure 12A,B, respectively. As shown in Figure 10A, the activity of HCl-treated T sand catalyst decreased to 67.4% ± 3.8% after the 10th usage of the first cycle. Upon the first regeneration, it increased to 95.2% ± 2.1% and decreased to 64.3% ± 4.6% after the 10th usage of the second cycle. Regeneration of the P sand catalyst is presented in Figure 10B and shows that after the first cycle of 10 uses, its activity dropped to 64.6% ± 4.8%, but upon the first regeneration activity increased to 98.4% ± 1.2% and dropped to 60.9% ± 3.8% at the end of second cycle of 10 uses. It is therefore apparent that both T and P sand can be used as catalysts for up to 50 times in a row without loss of conversion and can be regenerated after every 10 consecutive uses to recover activity in excess of 90% with every regeneration.

The regeneration studies of T-PEI^+ and P-PEI^+ catalysts were performed at similar conditions as mentioned earlier, but this time each cycle consisted of five consecutive catalytic reactions (instead of 10), although again the catalysts were subjected to four regenerations. The findings are shown in Figure 10C,D, respectively. The activities of each catalyst in the first and fifth reaction of each cycle during the four regenerations are shown in Figure 10C,D.

As shown in Figure 10C, the activity of T-PEI^+ decreased to 56.9% ± 2.9% after the fifth usage of the first cycle and increased to 103.5% ± 1.7% after the first regeneration, before decreasing to 60.8% ± 3.1% after the fifth use of the second cycle. The regeneration graphs of P-$PEI^+$are shown in Figure 10D. Interestingly, P-PEI^+ catalysts showed less activity loss than T-PEI^+ during each cycle. Regardless, both T-PEI^+ and P-PEI^+ sand catalysts can be used up to 25 times in a row maintaining 100 conversion capability and can be consistently

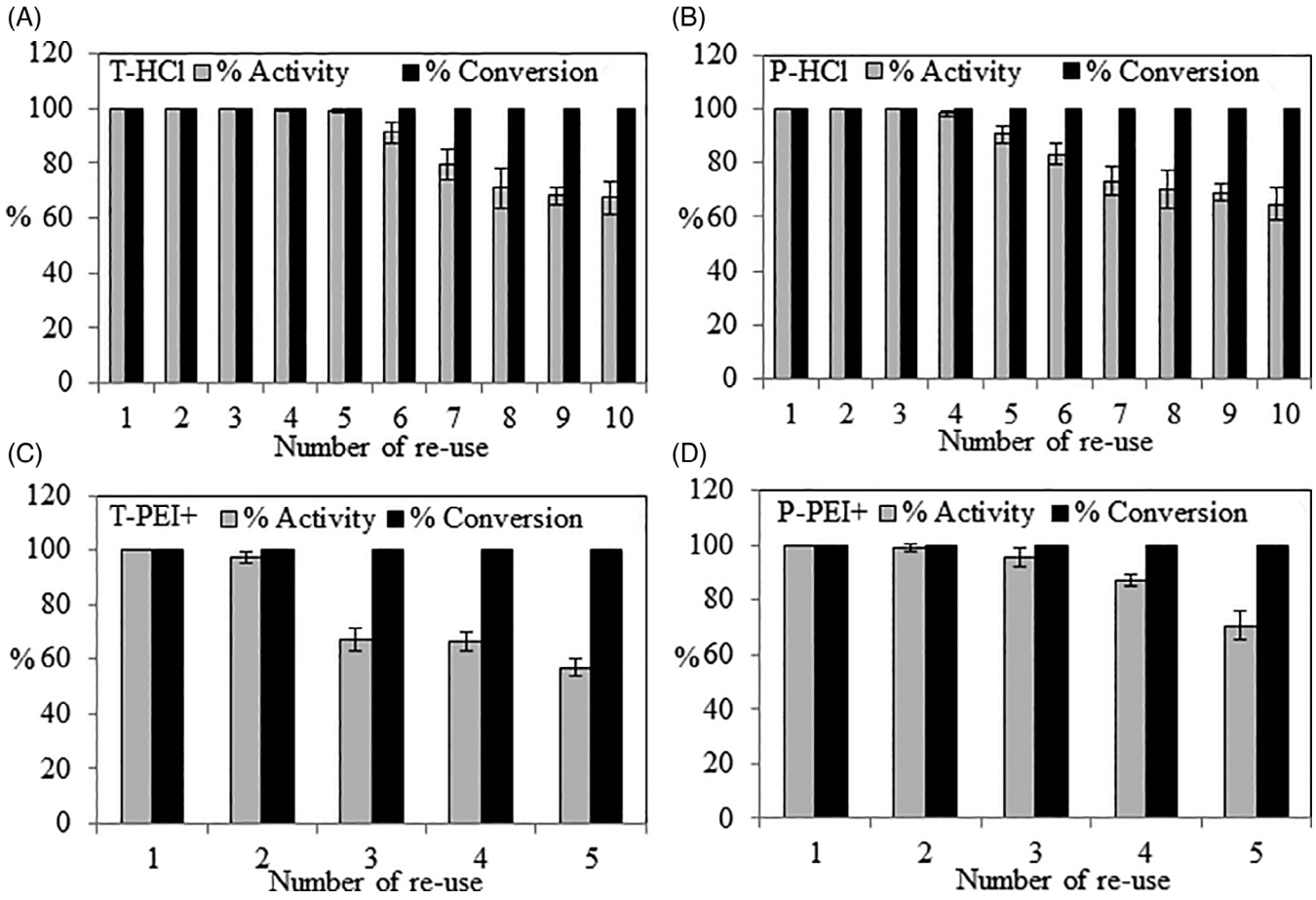

FIGURE 9 Reusability of A, HCl-treated, *T*(T-HCl); B, HCl-treated P, (P-HCl); C, T-PEI+; and D, P-PEI+ sand samples as catalysts for the NaBH4 dehydrogenation reaction in methanol (Catalyst: 50 mg, 20 mL methanol, 25°C, 1000 rpm mixing rate)

regenerated after every five sequential uses to regain activity of over 98%, hence losing less than 30% of their activity by the end of the fifth use of each cycle.

The formation of $NaB(OCH_3)_4$ as a reaction byproduct on the surface of the sand catalysts was confirmed with FT-IR analysis. The FT-IR spectra of unused T and P sand samples and those after the 10th use were compared, as shown in Figure 11A,B, respectively.

The newly appearing peaks at 1437 and 1330 cm^{-1} can be assigned to C—H stretching and characteristic B—O peaks, respectively, for T sand catalyst used 10 times in a row. Similar peaks at 1441 and 1337 cm^{-1} were also observed in the FT-IR spectrum of P sand catalyst after 10 uses. The regeneration of the sand catalysts was also confirmed via FT-IR spectra of T and P sand samples washed with 1M HCl after their 10th use. Clearly, the peaks generated from $NaB(OCH_3)_4$ at around 1430 to 1440 and 1330 to 1340 cm^{-1} disappeared after the acid wash for both T and P sand catalysts. As a result, the sand catalysts can be readily reusable and can be regenerated by mere HCl treatment providing additional advantages over conventional metal-based catalysts that are expensive, often toxic, prone to deactivation, and regeneration involves, more extensive treatment.

Similarly, the formation of $NaB(OCH_3)_4$ on the surface T-PEI^+ and P-PEI^+ catalysts was confirmed by FT-IR analysis, as shown in Figure 12A,B. Spectral analysis of the unused, five times used, and regenerated T-PEI^+ and P-PEI^+ catalysts are shown in Figure 12A,B, respectively.

The newly generated peaks at 1327 and 1327 $cm^{-1}$are characteristic of the B—O bond[54,55] in $B(OCH_3)_4^-$ for T-PEI^+ and P-PEI^+ sand catalysts, respectively, after the fifth use. Regeneration carried out with 1M HCl resulted in the disappearance of the B—O FT-IR peaks and a concomitant increase in catalytic activity, as the surface of the catalyst was freed from the dehydrogenation byproduct. Therefore, T-PEI^+ and P-PEI^+ sands can be practically reused and regenerated several times as catalysts for hydrogen production.

T and P sand samples, their corresponding PEI modified and protonated forms as well as five times consecutively used T-PEI^+ and P-PEI^+catalysts in $NaBH_4$ methanolytic dehydrogenation reaction were

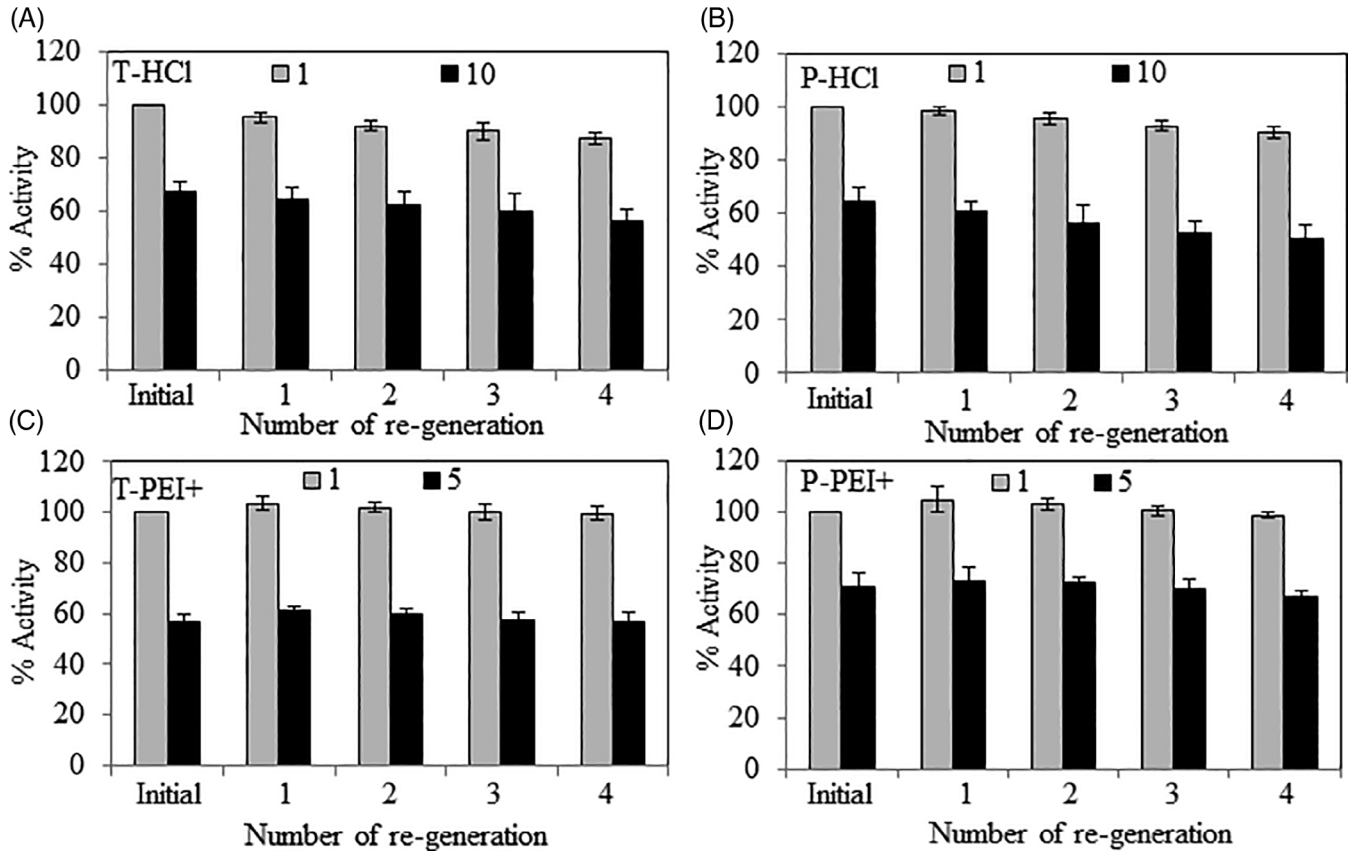

FIGURE 10 Regeneration studies of A, HCl-treated T, (T-HCl); B, HCl-treated P, (P-HCl); C, T-PEI+; and D, P-PEI+ sand samples as catalysts for NaBH4 dehydrogenation in methanol (Catalyst: 50 mg, 20 mL methanol, 25°C, 1000 rpm mixing rate)

characterized by XRD analysis and corresponding XRD spectra were given in Figure 13.

According to XRD patterns of five times used forms of T-PEI$^+$ and P-PEI$^+$ sand catalysts given in Figure S7A,B, the observed natrite peaks accompanies to quartz character of T-PEI$^+$, and P-PEI$^+$ sand catalysts, respectively. Accordingly, 3.1% and 1.54% natrite contents were observed at 3.41, 3.22, 2.96, 2.54, 2.36, and 2.25^{o}A, based upon reference spectra of natrite obtained from COD, database code 9009418. Moreover, the amorphous content of T-PEI$^+$ decreased from 49.6% to 28.8% and from 16.3% to 11.1% for P-PEI$^+$ catalysts upon five times sequential usage in methanolytic dehydrogenation of $NaBH_4$. From the obtained results, the quartz% of T-PEI$^+$ catalyst was observed to increase from 50.4% to 68.1% after five times successive usage in $NaBH_4$ dehydrogenation reaction in methanol, whereas amorphous% of PEI$^+$ structure on T sand sample decreased from 49.6% to 28.8% with 3.1% natrite formation. Similarly, the quartz% of P-PEI$^+$ catalyst increased from 83.7% to 87.4% after five times sequential usage in methanolytic dehydrogenation reaction of $NaBH_4$, whereas amorphous% of PEI$^+$ structure on P sand sample decreased from 16.3% to 11.1% with the 1.5% natrite formation. As can be clearly seen, the repetitive usage of both T-PEI+, and P-PEI+ catalysts in methanolytic NaBH4 dehydrogenation reaction decreased the amorphous content of catalysts with a consequent increase on total quartz % of catalysts. As it can be inferred from the XRD results, both T-PEI+ and P-PEI + sand catalysts somehow lost some portions of their amorphous contents during five times repetitive usage in methanolytic dehydrogenation reaction of NaBH4 that have led to consequent increase of the total quartz contents in the overall catalyst structures. The amorphous content (PEI$^+$) of the T-PEI$^+$ sand catalysts were decreased from 49.6% to 28.8% which in turn resulted in an increase on total quartz % in the overall structure of sand catalysts from 50.4% to 68.1% with 3.1% natrite formation. In a similar line, amorphous content of P-sand catalysts was decreased from 16.3% to 11.1% that gave rise to increase of the total quartz% from 83.7% from 87.4% with 1.5% natrite formation. It is noteworthy to address that T-PEI$^+$ and P-PEI$^+$ sand catalysts retained more than 58% and 68% of their amorphous contents after five times of sequential use in NaBH4 dehydrogenation reaction in methanol hence that implies further usability of these catalysts in more than five times usage as they also preserved respectively more than 56% and 70% of their

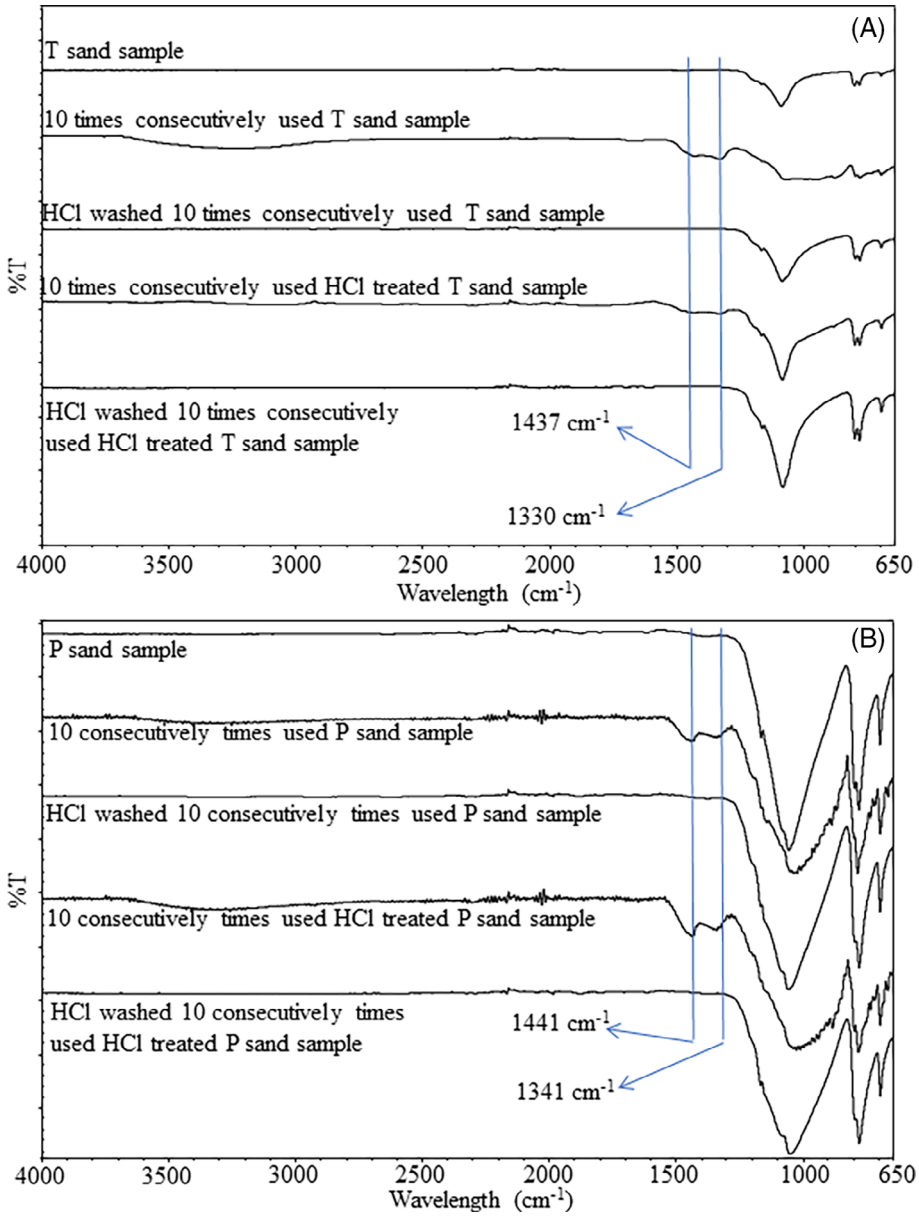

FIGURE 11 The FT-IR spectra of bare and HCl treated (A) T, and (B) P sand samples before and after 10th usage in methanolysis of NaBH4 reaction as catalyst [Colour figure can be viewed at wileyonlinelibrary.com]

catalytic activity with 100% conversion at the end of fifth usage. Also, these findings implicates better reusability performances of P-PEI$^+$ than the T-PEI$^+$ sand catalysts which can be justified in other words as P-PEI$^+$ catalysts are more stable than T-PEI$^+$ on preserving their percentile amorphous contents, hence it can potentially serve more than T-PEI$^+$ sand catalysts in successive utilizations.

3.6 | Figure of merit for $NaBH_4$ dehydrogenation in the presence of catalyst

The figure of merit (FOM) for the catalysts is defined as rate of hydrogen generation per unit molar concentration of $NaBH_4$ per unit weight of the catalyst. It is expressed in units of $l/(min.[NaBH_4].g_{cat})$.[56] The FOM analysis was done for the sand catalysts used in this study andtheir catalytic performances were compared with similar studies in literature and summarized in Table 2. The FOM values for T-PEI$^+$, and P-PEI$^+$ catalyst are found to be better than those for the T-HCl and P-HCl catalysts with no surprise, and the calculated FOM values are 69.6, 57.1, 10.0, and 8.9 $L/(min.[NaBH_4].g_{cat})$, respectively. Even, the FOM values of SiO_2-HCl particles calculated from the reported study[21] is better than the HCl-treated T and P catalysts with 11.4 $L/(min.[NaBH_4].g_{cat})$, the PEI modification and subsequent protonation of T and P sand samples have increased the FOM values up to 69.6, and 57.1 $L/(min.[NaBH_4].g_{cat})$, respectively. Moreover, the obtained FOM values for T-PEI$^+$, and P-PEI$^+$ catalysts

were found to be better than some of the reported catalysts in literature for $NaBH_4$ dehydrogenation reaction such as 0.6 L/(min.[$NaBH_4$].g_{cat}) for Ru_5Co/C catalyst,[31] 22.7 L/(min.[$NaBH_4$].g_{cat}) for SO_4^{2-}/CuO catalyst,[52] 16.0 L/(min.[$NaBH_4$].g_{cat}) for p(2-VP)$^{++}C_6$ catalyst,[35] 43.8 L/(min.[$NaBH_4$].g_{cat}) for Ni_2P-TOP catalyst,[37] 53.3 L/(min.[$NaBH_4$].g_{cat}) for Cell-EPC-DETA-HCl catalyst,[40] 10.2 L/(min.[$NaBH_4$].g_{cat}) for CF-A-CH catalyst,[48] and 8.3 L/(min.[$NaBH_4$].g_{cat}) for Ag@CFC catalyst,[53] respectively.

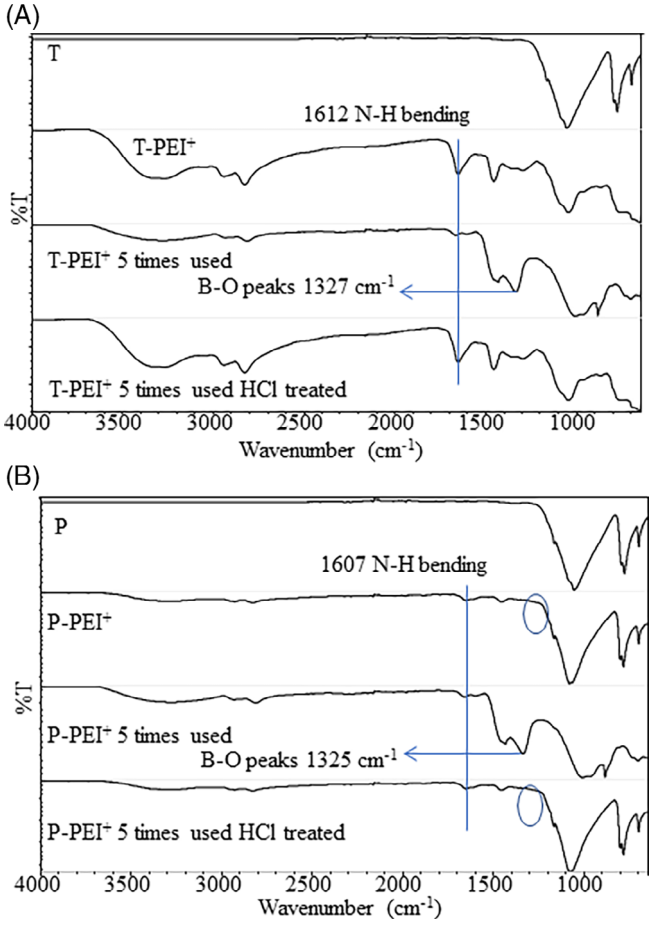

FIGURE 12 The FT-IR spectra of bare and HCl treated (A) T-PEI+, and (B) P-PEI+ sand samples before and after fifth usage in methanolysis of NaBH4 reaction as catalyst [Colour figure can be viewed at wileyonlinelibrary.com]

4 | CONCLUSIONS

The study has shown that natural sands collected from Tampa (T) and Panama City (P) beaches can be successfully used as catalysts for the $NaBH_4$ dehydrogenation reaction in methanol. As expected, the smallest sizes of T and P sand samples (<250 μm) showed better catalytic activity that the coarser sizes by achieving hydrogen production (HBR) from $NaBH_4$ of 565 ± 18, and 482 ± 24 mL H_2 (min.g of catalyst)$^{-1}$, respectively. To increase HGR, T and P sand samples were treated with NaOH and various common acids as a means of increasing the number of hydroxyl groups on the catalyst surface. HCl treatment, the most effective one, enhanced the performance of T and P sand samples to 705 ± 51, and 690 ± 47 mL H_2 (min.g of catalyst)$^{-1}$, respectively. The catalytic activities of T and P sand samples were further increased upon PEI modification and protonation, reaching 4408 ± 187, and 3879 ± 169 mL H_2 (min.g of catalyst)$^{-1}$ for T-PEI$^+$ and P-PEI$^+$, respectively, which are comparable to or better than several metal-based catalysts. The activation energy Eaof HCl-treated T and P sand samples was 24.6 and 25.9 kJ/mol, respectively, which are better (lower) than most metal and non-metal-based catalysts of $NaBH_4$ dehydrogenation in methanol reported in the literature. Interestingly, the E_a values of T-PEI$^+$, and P-PEI$^+$were higher than HCl-treated T and P catalysts (36.1 and 36.6 kJ/mol, respectively), although they exhibited higher catalytic activity. During each of

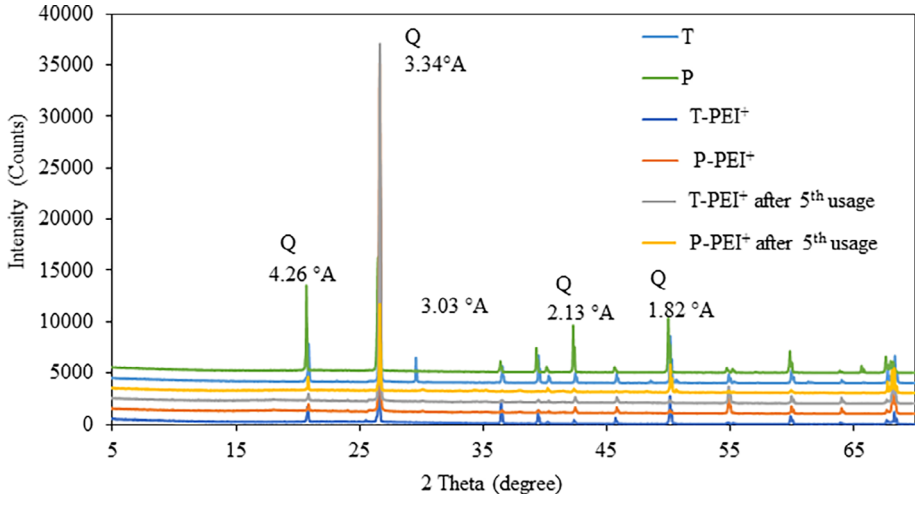

FIGURE 13 The comparison of XRD patterns of T and P based catalysts [Colour figure can be viewed at wileyonlinelibrary.com]

10 consecutive uses, HCl-treated T and P sand samples achieved 100% conversion and suffered less than 30% reduction in activity. Remarkably, simple regeneration with HCl fully restored the activity of both T and P sand catalysts. Reusability and regeneration were also demonstrated for T-PEI$^+$ and P-PEI$^+$, although not as effectively as for HCl-treated T and P sand samples. In summary, naturally abundant, sustainable, and inexpensive sand from the coasts of Florida can act as an effective catalyst for HBR from $NaBH_4$ in methanol, potentially displacing costly and often toxic metal catalysts to serve the needs of clean energy production. The promise of using natural sand as a renewable energy (hydrogen) production catalyst was reinforced by the ability to reuse and regenerate the sand's catalytic activity, thus significantly extending its value.

ACKNOWLEDGEMENT

The authors greatly acknowledge for the support provided by Yildiz Yildirim for XRD studies.

DATA AVAILABILITY STATEMENT

The data that supports the findings of this study are available in the supplementary material of this article.

ORCID

Nurettin Sahiner https://orcid.org/0000-0003-0120-530X

REFERENCES

1. Dellano-Paz F, Calvo-Silvosa A, Iglesias Antelo S, Soares I. The European low carbon mix for 2030: the role of renewable energy sources in an environmentally and socially efficient approach. *Renew Sustain Energy Rev*. 2015;48:49-61. https://doi.org/10.1016/j.rser.2015.03.032.
2. Sarkar A, Banerjee R. Net energy analysis of hydrogen storage options. *Int J Hydrogen Energy*. 2005;30:867-877. https://doi.org/10.1016/j.ijhydene.2004.10.021.
3. Lee J, Shin H, Choi KS, Lee J, Choi JY, Yu HK. Carbon layer supported nickel catalyst for sodium borohydride ($NaBH_4$) dehydrogenation. *Int J Hydrogen Energy*. 2019;44:2943-2950. https://doi.org/10.1016/j.ijhydene.2018.11.218.
4. Mao J, Gregory D. Recent advances in the use of sodium borohydride as a solid-state hydrogen store. *Energies*. 2015;8:430-436. https://doi.org/10.3390/en8010430.
5. Allakhverdiev SI. Photosynthetic and biomimetic hydrogen production. *Int J Hydrogen Energy*. 2012;37:8744-8752. https://doi.org/10.1016/j.ijhydene.2012.01.045.
6. Singh R, Dutta S. A review on H_2 production through photocatalytic reactions using TiO_2/TiO_2-assisted catalysts. *Fuel*. 2018;220:607-620. https://doi.org/10.1016/j.fuel.2018.02.068.
7. Wang Y, Shen Y, Qi K, Cao Z, Zhang K, Wu S. Nanostructured cobalt-phosphorous catalysts for hydrogen generation from hydrolysis of sodium borohydride solution. *Renew Energy*. 2016;89:285-294. https://doi.org/10.1016/j.renene.2015.12.026.
8. Fiorenza R, Scire S, Venezia AM. Carbon supported bimetallic Ru-Co catalysts for H_2 production through $NaBH_4$ and NH_3BH_3 hydrolysis. *Int. J. Energ. Res.* 2018;42:1183-1195. https://doi.org/10.1002/er.3918.
9. Matsunaga T, Buchter F, Miwa K, Towata S, Orimo S, Züttel A. Magnesium borohydride: a new hydrogen storage material. *Renew Energy*. 2008;33:193-196. https://doi.org/10.1016/j.renene.2007.05.004.
10. Fan MQ, Liu S, Sun WQ, Fei Y, Pan H, Shu KY. Controllable hydrogen generation and hydrolysis mechanism of AlLi/$NaBH_4$ system activated by $CoCl_2$ solution. *Renew Energy*. 2012;46:203-209. https://doi.org/10.1016/j.renene.2012.03.028.
11. Li X, Zhang Q, Luo M, Yao Q, Lu Z-H. Ultrafine Rh nanoparticles confined by nitrogen-rich covalent organic frameworks for methanolysis of ammonia borane. *Inorg Chem Front*. 2020;7:1298-1306. https://doi.org/10.1039/d0qi00073f.
12. Li H, Yan Y, Feng S, et al. Hydrogen release mechanism and performance of ammonia borane catalyzed by transition metal catalysts Cu-Co/MgO (100). *Int J Energ Res*. 2019;43:921-930. https://doi.org/10.1002/er.4325.
13. Wang K, Yao Q, Qing S, Lu Z-H. $La(OH)_3$ nanosheet-supported CoPt nanoparticles: a highly efficient and magnetically recyclable catalyst for hydrogen production from hydrazine in aqueous solution. *J Mater Chem A*. 2019;7:9903-9911. https://doi.org/10.1039/c9ta01066a.
14. Azad A-M, Kesavan S, Al-Batty S. A closed-loop proposal for hydrogen generation using steel waste and a prototype solar concentrator. *Int. J. Energ. Res.* 2009;33:481-498. https://doi.org/10.1002/er.1491.
15. Yao Q, Yang K, Nie W, Li Y, Lu Z-H. Highly efficient hydrogen generation from hydrazine borane via a MoO_x-promoted NiPd nanocatalyst. *Renew Energy*. 2020;147:2024-2031. https://doi.org/10.1016/j.renene.2019.09.144.
16. Moussa G, Moury R, Demirci UB, Şener T, Miele P. Boron-based hydrides for chemical hydrogen storage. *Int. J. Energ. Res.* 2013;37:825-842. https://doi.org/10.1002/er.3027.
17. Martelli P, Caputo R, Remhof A, Mauron P, Borgschulte A, Züttel A. Stability and decomposition of $NaBH_4$. *J Phys Chem C*. 2010;114:7173-7177. https://doi.org/10.1021/jp909341z.
18. Demirci UB, Miele P. Sodium borohydride versus ammonia borane, in hydrogen storage and direct fuel cell applications. *Energ Environ Sci*. 2009;2:627-637. https://doi.org/10.1039/B900595A.
19. Wee JH, Lee KY, Kim SH. Sodium borohydride as the hydrogen supplier for proton exchange membrane fuel cell systems. *Fuel Process Technol*. 2006;87:811-819. https://doi.org/10.1016/j.fuproc.2006.05.001.
20. Budroni MA, Garroni S, Mulas G, Rustici M. Bursting dynamics in molecular hydrogen generation via sodium borohydride hydrolysis. *J Phys Chem C*. 2017;121:4891-4898. https://doi.org/10.1021/acs.jpcc.6b12797.
21. Sahiner N, Yasar AO. A new application for colloidal silica particles: natural, environmentally friendly, low-cost, and reusable catalyst material for H_2 production from $NaBH_4$ methanolysis. *Ind Eng Chem Res*. 2016;55:1245-11252. https://doi.org/10.1021/acs.iecr.6b03089.
22. Ould-Amara H, Alligier D, Petit E, Yot PG, Demirci UB. Sodium borohydride and propylene glycol, an effective combination for the generation of 2.3 wt% of hydrogen. *Int J*

Hydrogen Energy. 2018;43:237-7244. https://doi.org/10.1016/j.ijhydene.2018.02.169.

23. Arzac GM, Fernández A. Hydrogen production through sodium borohydride ethanolysis. *Int J Hydrogen Energy*. 2015;40:5326-5332. https://doi.org/10.1016/j.ijhydene.2015.01.115.
24. Yang BC, Chai YJ, Yang FL, Zhang Q, Liu H, Wang N. Hydrogen generation by aluminum-water reaction in acidic and alkaline media and its reaction dynamics. *Int. J. Energ. Res.* 2018;42:1594-1602. https://doi.org/10.1002/er.3953.
25. Tahir MB, Riaz KN, Asiri AM. Boosting the performance of visible light-driven WO_3/g-C_3N_4 anchored with $BiVO_4$ nanoparticles for photocatalytic hydrogen evolution. *Int. J. Energ. Res.* 2019;43:5747-5758. https://doi.org/10.1002/er.4673.
26. Tahir MB, Nabi G, Rafique M, Khalic NR. Role of fullerene to improve the WO_3 performance for photocatalytic applications and hydrogen evolution. *Int. J. Energ. Res.* 2018;42:4783-4789. https://doi.org/10.1002/er.4231.
27. Wang H, Xu J, Sheng L, Liu X, Lu Y, Li W. A review on biohydrogen production technology. *Int. J. Energ. Res.* 2018;42:3442-3453. https://doi.org/10.1002/er.4044.
28. Lo CTF, Karan K, Davis BR. Kinetic studies of reaction between sodium borohydride and methanol, water, and their mixtures. *Ind. Eng. Chem. Res.* 2007;4:5478-5484. https://doi.org/10.1021/ie0608861.
29. Ocon JD, Tuan TN, Yi Y, De Leon RL, Lee JK, Lee J. Ultrafast and stable hydrogen generation from sodium borohydride in methanol and water over Fe-B nanoparticles. *J Power Sources*. 2013;243:444-450. https://doi.org/10.1016/j.jpowsour.2013.06.019.
30. Hannauer J, Demirci UB, Pastor G, Geantet C, Herrmann JM, Miele P. Hydrogen release through catalyzed methanolysis of solid sodium borohydride. *Energ Environ Sci*. 2010;3:1796-1803. https://doi.org/10.1039/C0EE00023J.
31. Wang FH, Wang YN, Zhang YJ, Luo YM, Zhu H. Highly dispersed RuCo bimetallic nanoparticles supported on carbon black: enhanced catalytic activity for hydrogen generation from $NaBH_4$ methanolysis. *J Mater Sci*. 2018;53:6831-6841. https://doi.org/10.1007/s10853-018-2013-1.
32. Wang F, Zhang Y, Wang Y, Luo Y, Chen Y, Zhu H. Co-P nanoparticles supported on dandelion-like CNTs-Ni foam composite carrier as a novel catalyst for hydrogen generation from $NaBH_4$ methanolysis. *Int J Hydrogen Energy*. 2018;43:8805-8814. https://doi.org/10.1016/j.ijhydene.2018.03.140.
33. Yao Q, Ding Y, Lu ZH. Noble-metal-free nanocatalyst for hydrogen generation from boron- and nitrogen-based hydrides. *Inorg. Chem. Front*. 2020. https://doi.org/10.1039/D0QI00766H.
34. Xu D, Zhang Y, Cheng F, Zhao L. Enhanced hydrogen generation by methanolysis of sodium borohydride in the presence of phosphorus modified boehmite. *Fuel*. 2014;134:257-262. https://doi.org/10.1016/j.fuel.2014.05.071.
35. Sahiner N, Yasar AO, Aktas N. Metal-free pyridinium-based polymeric ionic liquids as catalyst for H_2 generation from $NaBH_4$. *Renew Energy*. 2017;101:1005-1012. https://doi.org/10.1016/j.renene.2016.09.066.
36. Wang F, Luo Y, Wang Y, Zhu H. The preparation and performance of a novel spherical spider web-like structure Ru-Ni/Ni foam catalyst for $NaBH_4$ methanolysis. *Int J Hydrogen Energy*. 2019;44:13185-13194. https://doi.org/10.1016/j.ijhydene.2019.01.123.
37. Yan K, Li Y, Zhang X, et al. Effect of preparation method on Ni_2P/SiO_2 catalytic activity for $NaBH_4$ methanolysis and phenol hydrodeoxygenation. *Int J Hydrogen Energy*. 2015;40:16137-16146. https://doi.org/10.1016/j.ijhydene.2015.09.145.
38. Sahiner N, Sengel SB. Various amine functionalized halloysite nanotube as efficient metal free catalysts for H_2 generation from sodium borohydride methanolysis. *Appl Clay Sci*. 2017;146:517-525. https://doi.org/10.1016/j.clay.2017.07.008.
39. Vinokurov V, Stavitskaya A, Glotov A, et al. Halloysite nanotube-based cobalt mesocatalyst for hydrogen production from sodium borohydride. *J Solid State Chem*. 2018;268:182-189. https://doi.org/10.1016/j.jssc.2018.08.042.
40. Sahiner N, Demirci S. Natural microgranular cellulose as alternative catalyst to metal nanoparticles for H_2 production from $NaBH_4$ methanolysis. *Appl.Catal. B Environ.* 2017;202:199-206. https://doi.org/10.1016/j.apcatb.2016.09.028.
41. Sahiner N. Carbon spheres from lactose as green catalyst for fast hydrogen production via methanolysis. *Int J Hydrogen Energy*. 2018;43:9687-9695.
42. Young RA. Introduction to Rietveld method. In: Young RA, ed. *International union of crystallography*. Oxford: Oxford Press; 1995:1-38.
43. Davis RE, Gottbrath JA. Boron hydrides. V. Methanolysis of sodium borohydride. *J Am Chem Soc*. 1962;84:895-898. https://doi.org/10.1021/ja00865a003.
44. Balbay A, Saka C. Effect of phosphoric acid and acetic acid addition on the hydrogen evolution using Ni based catalyst prepared in ethanol, methanol, and water solvents. *Energ Source Part A*. 2018;40:2442-2450. https://doi.org/10.1080/15567036.2018.1502841.
45. Guella G, Zanchetta C, Patton B, Miotello A. New insights on the mechanism of palladium-catalyzed hydrolysis of sodium borohydride from ^{11}B NMR measurements. *J Phys Chem B*. 2006;110:17024-17033. https://doi.org/10.1021/jp063362n.
46. Peña-Alonso P, Sicurelli A, Callone E, Carturan G, Raj R. A picoscale catalyst for hydrogen generation from $NaBH_4$ for fuel cells. *J. Power Source*. 2007;165:315-323. https://doi.org/10.1016/j.jpowsour.2006.12.043.
47. Liu CH, Chen BH, Hsueh CL, Ku JR, Tsau F, Hwang KJ. Preparation of magnetic cobalt-based catalyst for hydrogen generation from alkaline $NaBH_4$ solution. *Appl Catal B Environ*. 2009;91:368-379. https://doi.org/10.1016/j.apcatb.2009.06.003.
48. Ali F, Khan SB, Asiri AM. Chitosan coated cellulose cotton fibers as catalyst for the H_2 production from $NaBH_4$ methanolysis. *Int J Hydrogen Energy*. 2019;44:4143-4155. https://doi.org/10.1016/j.ijhydene.2018.12.158.
49. Xu D, Zhao L, Dai P, Ji S. Hydrogen generation from methanolysis of sodium borohydride over Co/Al_2O_3 catalyst. *J Nat Gas Chem*. 2012;21:488-494. https://doi.org/10.1016/S1003-9953(11)60395-2.
50. Su CC, Lu MC, Wang SL, Huang YH. Ruthenium immobilized on Al_2O_3 pellets as a catalyst for hydrogen generation from hydrolysis and methanolysis of sodium borohydride. *RSC Adv*. 2012;2:2073-2079. https://doi.org/10.1039/C2RA01233B.
51. Luo W, Cheng W, Hu M, et al. Ultrahigh catalytic activity of $_L$-Proline-functionalized Rh nanoparticles for methanolysis of

ammonia borane. *Chem Sus Chem*. 2019;12:535-541. https://doi.org/10.1002/cssc.201802157.

52. Xu D, Lai X, Guo W, Zhang X, Wang C, Dai P. Efficient catalytic properties of SO_4^{2-}/M_xO_y (M = Cu, Co, Fe) catalysts for hydrogen generation by methanolysis of sodium borohydride. *Int J Hydrogen Energy*. 2018;43:6594-6602. https://doi.org/10.1016/j.ijhydene.2018.02.074.
53. Ali F, Khan SB, Asiri AM. Enhanced H_2 generation from $NaBH_4$ hydrolysis and methanolysis by cellulose micro-fibrous cottons as metal template catalyst. *Int J Hydrogen Energy*. 2018;43:6539-6550. https://doi.org/10.1016/j.ijhydene.2018.02.008.
54. Peak D, Luther GW, Sparks DL. ATR-FT-IR spectroscopic studies of boric acid adsorption on hydrous ferric oxide. *Geochim Cosmochim Acta*. 2003;67:2551-2560.
55. Demirci S, Sunol AK, Sahiner N. Catalytic activity of amine functionalized titanium dioxide nanoparticles in methanolysis of sodium borohydride for hydrogen generation. *Appl Catal B*. 2020;261:118242. https://doi.org/10.1016/j.apcatb.2019.118242.
56. Hu L, Ceccato R, Raj R. Ultrahigh figure of merit for hydrogen generation from sodium borohydride using ternary metal catalysts. *J Power Source*. 2011;196:69-75. https://doi.org/10.1016/j.jpowsour.2010.07.037.

SUPPORTING INFORMATION

Additional supporting information may be found online in the Supporting Information section at the end of this article.

How to cite this article: Inger E, Demirci S, Can M, Sunol AK, Philippidis G, Sahiner N. PEI modified natural sands of Florida as catalysts for hydrogen production from sodium borohydride dehydrogenation in methanol. *Int J Energy Res*. 2020;1–20. https://doi.org/10.1002/er.6060